A COMPARATIVE STUDY OF COASTAL FRONTOGENESIS

by

DAVID ALAN CLARK

B.S., University of Lowell
(1981)

SUBMITTED TO THE DEPARTMENT OF
EARTH, ATMOSPHERIC, AND PLANETARY SCIENCES
IN PARTIAL FULFILLMENT OF THE
REQUIREMENTS FOR THE DEGREE OF

MASTER OF SCIENCE

at the

MASSACHUSETTS INSTITUTE OF TECHNOLOGY

September 1983

Signature of Author . . . . . .
Department of Earth, Atmospheric, and Planetary Sciences
September, 1983

Certified by . . . . . .
Frederick Sanders
Thesis Supervisor

Accepted by . . . . . .
Ronald G. Prinn
Chairman, Departmental Committee on Graduate Students

A COMPARATIVE STUDY OF COASTAL FRONTOGENESIS

by

DAVID ALAN CLARK

Submitted to the Department of Earth, Atmospheric, and Planetary Sciences in September 1983 in partial fulfillment of the requirements for the degree of Master of Science

ABSTRACT

Two cases of coastal frontogenesis along the Atlantic coastline are presented. The first case occurred on 23-24 January 1982 and involved the development of an extraordinarily intense lower boundary layer frontal zone along the coast of New England. The front was initiated by the presence of a cold anticyclone situated in northeastern Maine that provided onshore geostrophic flow along the coastline to the south. The second coastal front case occurred on 15 December 1981 and it involved a weak, migrating cyclone that was responsible for a local strengthening of the temperature gradient along the Atlantic coastline. The term "zipper low" is introduced to describe this type of low pressure system, as it has the effect of zipping up the surface isotherms as it progresses along the coast.

The two mechanisms for coastal frontogenesis are compared and contrasted. The flow associated with the cold anticyclone coastal front is found to be predominantly normal to the frontal zone, and its initiation and development appear to be independent of the effect of horizontal geostrophic deformation. The flow that accompanies the zipper low is more parallel to the frontal zone, and it appears that its associated horizontal geostrophic deformation plays a positive frontogenetical role in the observed strengthening of the thermal gradient.

Thesis Supervisor: Professor Frederick Sanders
Title: Professor of Meteorology

Table of Contents

List of Figures

List of Figures (Continued)

List of Figures (Continued)

1.0 Historical Background and Introduction

A description of the physical processes involved in the initiation and development of coastal fronts was formally introduced by Bosart, Vaudo, and Helsdon (1972). They described the coastal front as a mesoscale boundary layer phenomenon that is characterized by a large contrast in temperature over horizontal distances of 5 to 10 km on a length scale of more than 100 km. The strong temperature gradient is accompanied by a cyclonic wind shift across the front; onshore winds become strong at 10 to 20 m/s while the inland flow remains light and maintains a northerly component. It was observed that there is an enhancement of precipitation on the cold side of the front, and that the location of the frontal zone often delineates the transition from frozen to non-frozen precipitation.

Bosart *et al.* speculated that under appropriate synoptic conditions, coastal frontogenesis results from the combined effects of differential surface friction, irregular terrain, and a land-sea thermal contrast. They described the coastal front as a quasi-stationary phenomenon that forms locally to the south-southwest of a cold anticyclone. In the eastern United States, the anticyclone plays the role of funneling cold air southward to the east of the Appalachian Mountains. The cold air banked on the east side of the mountains is reflected hydrostatically by a ridging of the surface isobars, as

described by Baker (1970). As the anticyclone migrates eastward, the geostrophic flow over the ocean develops a strong easterly component. The differential friction between ocean and land results in a convergence of the onshore flow at the coastline and a corresponding convergence of the surface isotherms. This effect is greatest in the late fall and early spring when the temperature contrast between land and ocean is climatologically largest. The differential surface friction between ocean and land also aids in maintaining the ageostrophic northerly component of the inland wind. This effect was described by Lettau and Dabbert (1970) who stated that the boundary layer is very shallow when the inland wind strays more than 35 degrees from geostrophic, and the wind direction changes rapidly with height. They mention that such a situation could occur under conditions of extreme stability in which intense convergence would take place only in a shallow layer near the surface. Their description agrees with the observations associated with coastal fronts.

The introductory paper on coastal frontogenesis was followed by a climatological study by Bosart (1975). It revealed that the presence of a cold anticyclone was common to all coastal front cases considered. Evidence suggested that an anticyclone over Nova Scotia resulting in strong southeasterly geostrophic flow was most favorable for

coastal frontogenesis in the New England area. The study also revealed that an initial temperature gradient in excess of the climatological normal is necessary for the formation of a coastal front, and that the front forms locally as opposed to being transported inland from the Atlantic Ocean. The time scale for an order-of-magnitude increase in the horizontal temperature gradient was found to be one-half to one day, and this time depends upon the amount of differential diabatic heating. Another suggestion by the study is that the maximum horizontal geostrophic deformation occurs inland and coincides with the surface pressure ridge to the east of the Appalachian Mountains; this observation is crucial to the discussion of coastal fronts presented here.

Other authors have since considered various aspects of the coastal front phenomenon described by Bosart et al. Marks (1975) and Marks and Austin (1979) commented on the enhancement of precipitation that results from the presence of a coastal front. They claimed that such an enhancement is due to the creation of low clouds by the circulation associated with the front. These low clouds consist of cloud droplets that are eventually accreted by snowflakes which originate at higher levels, thus producing the observed enhancement of precipitation.

Ballentine (1980) developed a numerical model and used the data from Bosart et al. to test the relative

importance of the physical processes that were considered to be responsible for the initiation and maintenance of coastal frontogenesis. His conclusion was that the flux of heat from the ocean and its subsequent diffusion into the atmosphere is the major factor in the development of coastal fronts. He suggested that the effects of differential surface friction and latent heat release are secondary, and that the importance of the mountains in explaining the persistence of northerly winds just inland from the coast is questionable.

During the first decade since its introductory appearance in the literature, it had been generally accepted that the coastal front is a phenomenon whose initiation and maintenance is dependent upon onshore geostrophic flow normal to the front. The presence of a cold anticyclone to the north of the front has been considered to be a necessary ingredient for coastal frontogenesis, and the geostrophic deformation maximum coincident with its inland ridge has been dissociated with the formation of the front. Bosart (1975) conjectured that horizontal geostrophic deformation is incapable of initiating coastal frontogenesis. The present investigation, however, suggests that another mechanism for coastal frontogenesis exists, one in which geostrophic deformation may indeed play an important role. This

frontogenetical process is dependent upon the presence of a weak, migrating cyclone that is associated with a strengthening of the local temperature gradient. The term "zipper low" has been coined to describe such a cyclone, as it has the effect of zipping up the coastal temperature gradient as it progresses along the coast. In contrast to the coastal front description presented earlier, the flow associated with the zipper low remains more parallel to the coastline on the warm side of the front, and there appears to be a small, frontogenetically favorable area of horizontal geostrophic deformation that migrates in association with the low pressure system. This geostrophic deformation maximum usually appears ahead and to the left of the zipper low and is presumably associated with the initiation of frontogenesis.

This paper includes the documentation of an extraordinary case of coastal frontogenesis that occurred in New England on 23-24 January 1982. The intense frontal zone was induced by onshore flow to the south of a cold anticyclone. This case is followed by an example of frontogenesis associated with a zipper low that occurred on 15 December 1981. The two varying mechanisms for frontogenesis are compared and contrasted, including the characteristics and conditions that are typically associated with each.

2.0 Coastal Frontogenesis By A Cold Anticyclone: Case of 23-24 January 1982

The first case to be examined is one in which coastal frontogenesis is initiated in New England as the result of onshore geostrophic flow to the south of a cold anticyclone. The onset of the coastal front occurs just prior to 1200 GMT on 23 January 1982. The surface synoptic situation of the eastern United States at this time is shown in Figure 2.1. The most dominant feature of this map is an enormous cyclone centered between Lake Superior and Lake Michigan. This low has migrated northeastward from central Kansas in the previous 24 hours. Its movement was accompanied by a significant fall of central pressure of approximately 15 mb during the 24-hour period. The upper level support for this system is apparent in the deep cut-off low at 500 mb, shown in Figure 2.2. A second prominent feature of the surface map which is relevant to the ensuing coastal frontogenesis in New England is the cold anticyclone in northeastern Maine. It is situated at an ideal location for the development of a coastal front in New England, as suggested by the climatological study by Bosart (1975). A final noteworthy feature of Figure 2.1 is the weak surface circulation that is developing along the southern portion of the Carolina coast; this circulation appears as a 1018 mb low on the surface map. Note that a frontal zone lies along the Atlantic coastline as far north

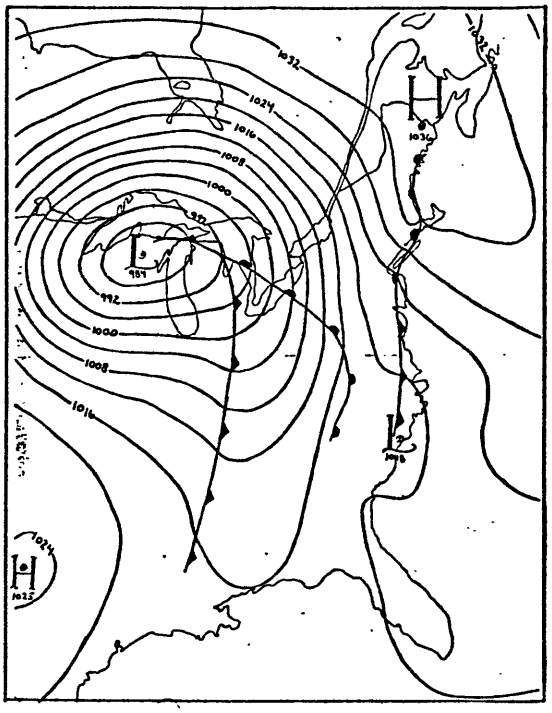

Figure 2.1 Surface pressure and frontal analysis for 1200 GMT 23 January 1982. Isobars are labeled in mb.

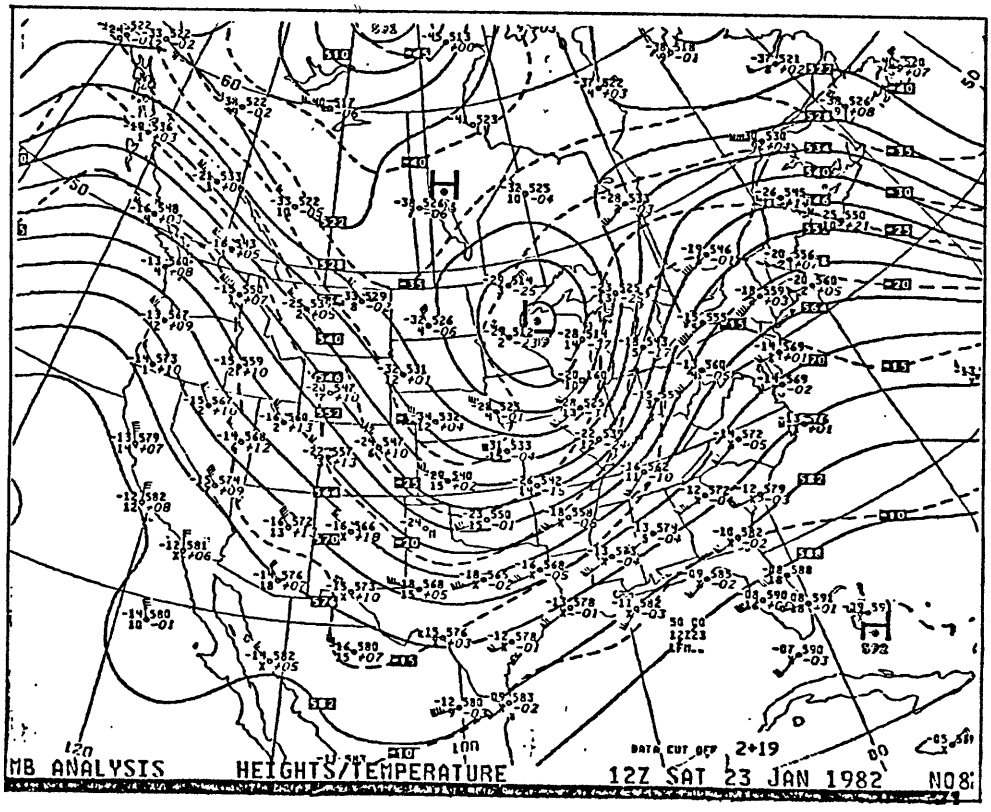

Figure 2.2 500 mb height analysis (dm) for 1200 GMT 23 January 1982. (from NMC)

as New England where the geostrophic flow is onshore. The fact that frontogenesis is occurring some 1500 km in advance of the small coastal disturbance suggests that the presence of the low itself is not playing a major role in the initiation of frontogenesis along the New England coastline. This low will, however, move rapidly northward and eventually contribute to the intensification of the New England coastal front, as well as to its ultimate dissipation.

We may now consider the development of the coastal front on a more local scale; Figure 2.3 is a map of New England indicating the location of useful observations. Included are the Coast Guard reporting stations just off the coastline. This map also includes the location of twelve key sites which are denoted by the letters A through L. These sites have been chosen as representative reference locations for deformation and frontogenesis calculations. Sites A through D represent atmospheric behavior inland; similarly, sites E through I represent behavior within the frontal zone along the coast, and sites J through L are representative of air over the ocean.

The local surface conditions just after the onset of the coastal front in New England (1200 GMT) are shown in Figure 2.4. The location of the front is denoted by a dashed line running along the coastline from Maine to Long Island. The prominent synoptic feature of this map is the

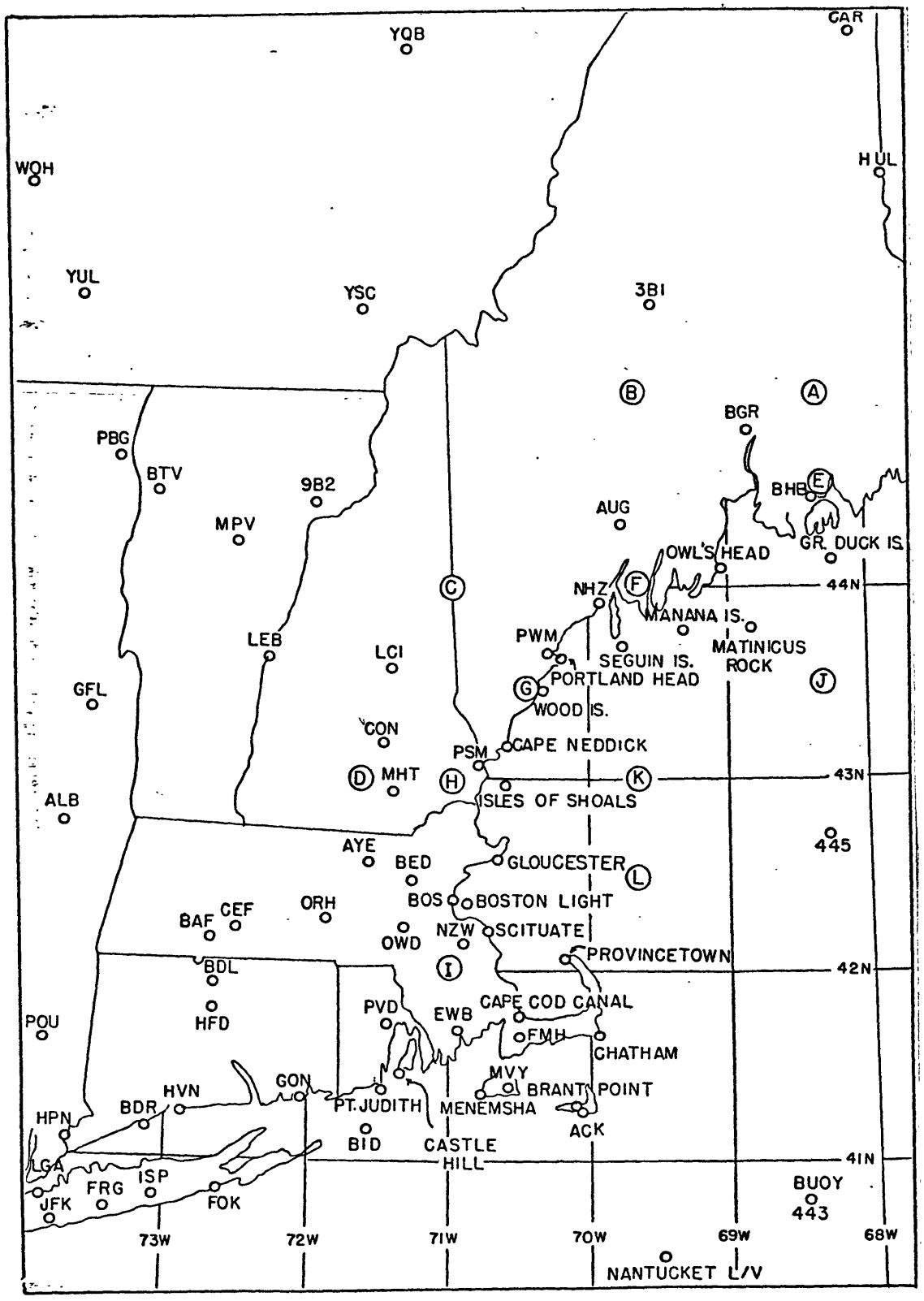

Figure 2.3 Locations of New England observing stations.

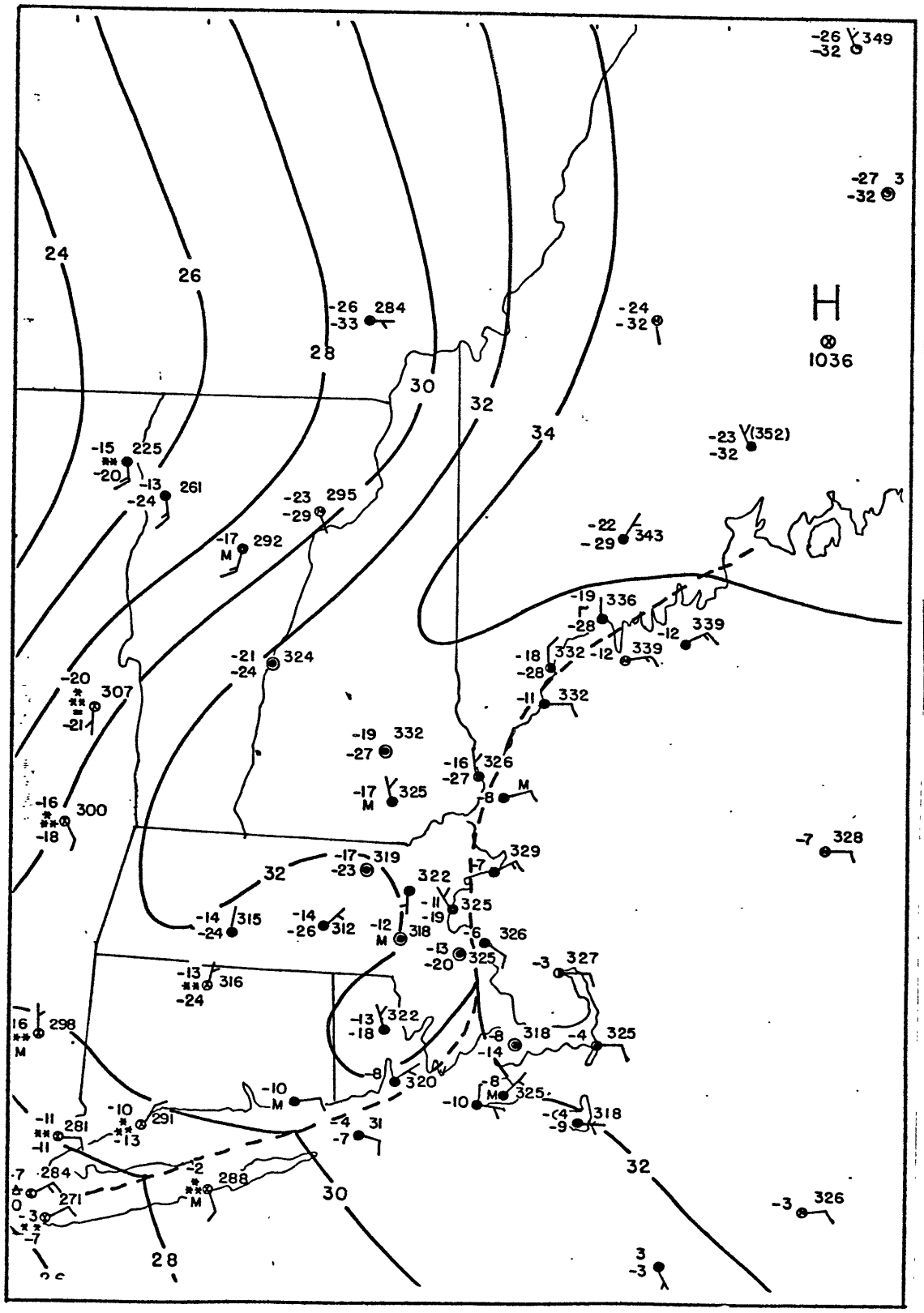

Figure 2.4 Surface analysis for 1200 GMT 23 January 1982. Isobars represent mb in excess of 1000. Temperatures in degrees Celsius. One full wind barb = 10 knots (approximately 5 m/s). Dashed line indicates location of coastal front.

cold 1036 mb anticyclone situated in northeastern Maine. The entire region is under the influence of the frigid air that has been ushered southward by this anticyclone and funneled to the east of the Appalachian Mountains. The clouds which cover the region did not move into central New England until after 0600 GMT which, coupled with the light winds inland, allowed for a considerable amount of radiational cooling overnight and a subsequent enhancement of the cold pocket of air in north central New England. This pocket of cold air is typical of coastal front situations in this area and Baker (1970) links it hydrostatically to the coinciding presence of the pressure ridge that exists to the east of the mountains. The overnight radiational cooling over land also aids in strengthening the land-sea contrast of air temperature. The sea surface temperatures from Maine to Long Island range from about -1° C to 3° C at this time, and the corresponding air temperatures over this water decrease to only -12°C to -2°C by 1200 GMT; meanwhile, the overnight cooling over land along the coast has allowed air temperatures to drop to a range of -22° C to -10° C from Maine to Long Island. This strengthening of the land-sea air temperature contrast has set up a "pre-coastal front" environment by 1200 GMT; Bosart (1975) claims that a local temperature gradient in excess of the climatological gradient exists in all coastal front cases yet studied, and

this criterion is certainly met in this particular case.

The surface wind field at 1200 GMT reveals that the formation of the coastal front is underway. Three hours earlier (the time resolution of the Coast Guard reports is 3 hours) the observed winds over the entire region were from the north and northwest, with local shifting to northeast at some isolated stations. By 1200 GMT, however, the majority of the Coast Guard stations are reporting winds with a strong easterly component, ranging from northeast to southeast at 3 to 8 m/s. Meanwhile, the wind over land remains light from the north and north-northwest.

Figure 2.5 shows the location of surface isotherms at 1200 GMT, as well as the dilatation axes of the observed horizontal deformation (i.e. deformation by the observed horizontal winds) at the twelve aforementioned key sites shown in Figure 2.3. Deformation calculations were made using a one degree latitude grid oriented east-west and north-south. The trough in the isotherms over north central New England illustrates the pocket of cold air that is banked on the east side of the Appalachians. The strongest temperature gradient runs along the coast from northern Massachusetts to the southern Maine coastline. The length of the dilatation axes on this map has been drawn proportional to the magnitude of the observed horizontal deformation. The deformation magnitudes are found to be relatively weak at the inland and ocean sites,

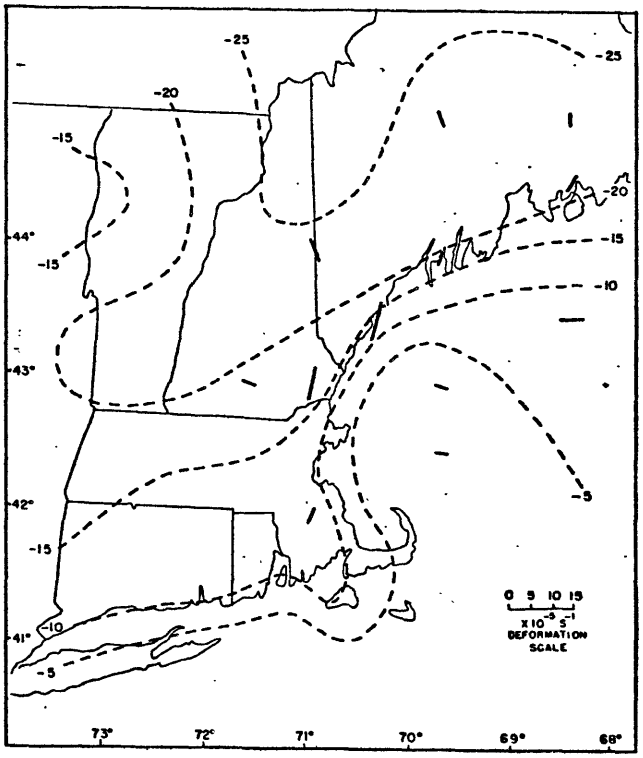

Figure 2.5 Surface isotherms (degrees Celsius) for 1200 GMT 23 January 1982. Axes indicate direction and magnitude of observed horizontal deformation calculated using a one degree latitude grid size.

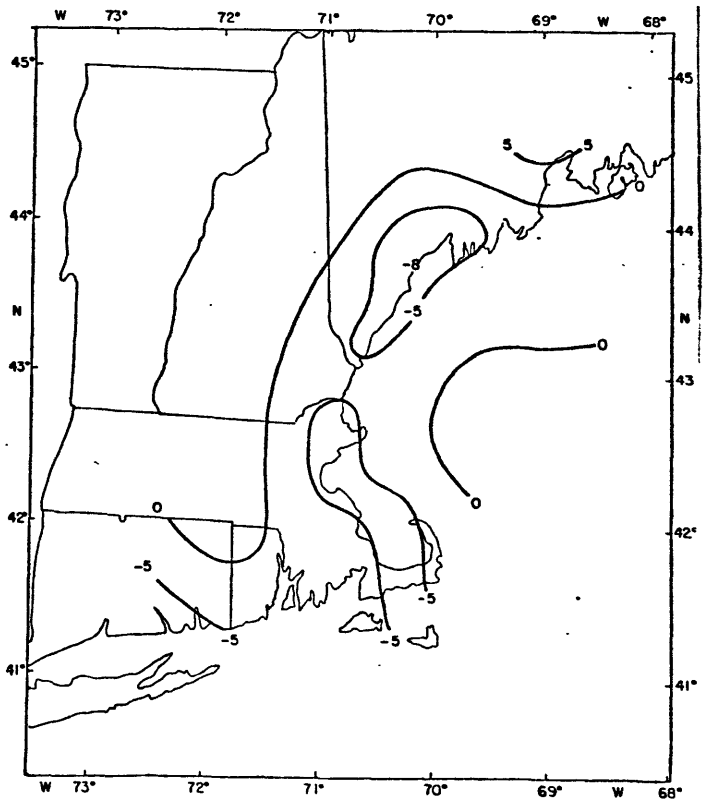

Figure 2.6 Observed horizontal divergence (10^{-5} s^{-1}) for 1200 GMT 23 January 1982. Values obtained using one degree latitude grid size.

while weak to moderate magnitudes are seen along the coast. The dilatation axes inland indicates that the deformation by the observed wind is acting in a frontolytical sense, as the angle they form with the surface isotherms is greater than 45 degrees (see Petterson, 1956). The dilatation axes at the coastal sites indicate frontogenetical deformation by the observed wind. Over the ocean, there appears to be frontogenesis at Sites J and K with frontolysis at Site L, but the magnitudes of deformation are relatively small and probably not very significant.

Figure 2.6 is a map illustrating the observed surface horizontal divergence at 1200 GMT. Calculations were made using a grid size of one degree latitude. The most noteworthy feature of the figure is the line of convergence that runs along the coast with a relative maximum of $-8 \times 10^{-5} s^{-1}$ located along the coastline of southern Maine. However, there is no precipitation reported in that area at this time, as precipitation in New England is restricted to light and moderate snow in western Connecticut. Also note that away from the coast, the horizontal surface wind is divergent both inland and over the ocean.

By 1800 GMT the coastal front has strengthened considerably (Figure 2.7) as temperature contrasts across the front at some locations are in excess of 10° C. The most intense portion of the front runs from Brunswick,

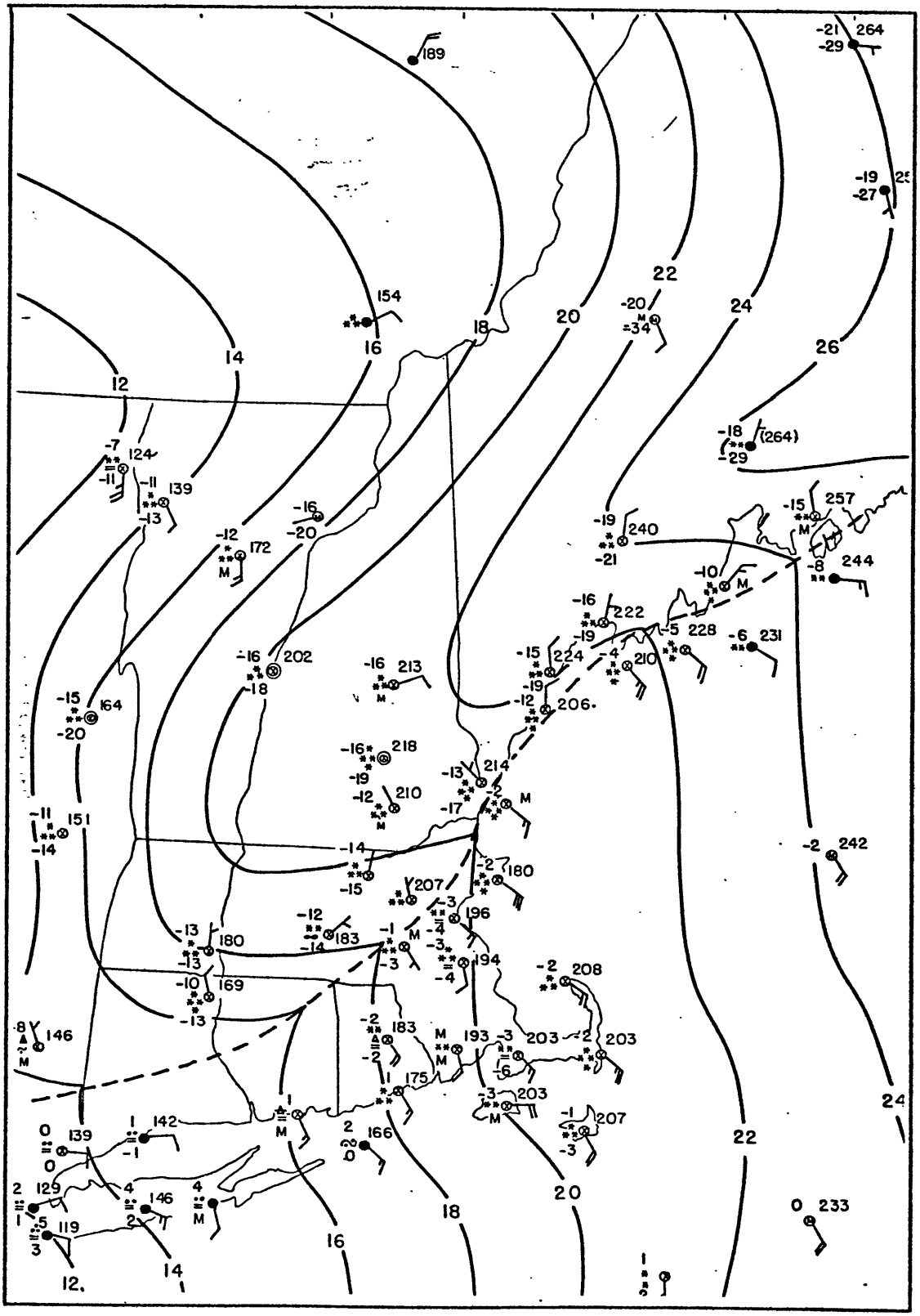

Figure 2.7 Surface analysis for 1800 GMT 23 January 1982.

Maine (NHZ) southward to the Gloucester Coast Guard station in northern Massachusetts. The land stations along this stretch of the coastline have reported a temperature increase of only 2 or 3°C during the past six hours, while the coast guard stations in this area have experienced a 5 to 7°C temperature jump over the same period. The exception to this is the Wood Island coast guard station which has gone from an easterly to a northerly wind accompanied by a 1°C temperature decrease over this period, indicating movement of the front slightly offshore at this time. The other coast guard stations are now reporting strong sustained winds out of the southeast at 7 to 15 m/s, while the flow on land along the coast remains from the north-northwest and north-northeast at the lighter clip of 2 to 5 m/s. Note also the backing of the wind at Portsmouth, New Hampshire (PSM) to northwesterly. The increased onshore flow over the ocean is the result of the strengthening of the pressure gradient over the entire area as the small coastal cyclone, which is now located in southern New Jersey, has deepened to 1008 mb and will soon be approaching New England. The elongated ridge remains inland as a reflection of the cold air piled to the east of the mountains, while there is a distinct kinking of the isobars along the front which is testimony to the sharpness of the frontal zone within the boundary layer.

The precipitation over most of New England began as

light snow starting between 1400 GMT and 1600 GMT; by 1800 GMT it has increased to moderate and heavy snow that is falling over much of the region, with heaviest intensities found where the coastal front is most pronounced. Freezing rain, ice pellets, and snow grains are falling on the warm side of the front in Rhode Island and eastern Connecticut at this time, indicating that a changeover from frozen to non-frozen precipitation is imminent.

Inspection of Figure 2.8 reveals the packing of the isotherms along the southern coast of Maine. The southern length of the front has moved inland and now runs from northeastern Massachusetts into central Connecticut. The observed horizontal deformation at the inland sites continues to work in a frontolytical sense with weak to moderate magnitudes, while along the coast the observed deformation has become moderate to strong and is acting in a strongly frontogenetical manner as the dilatation axes are nearly parallel to the surface isotherms. The observed deformation is weakest at the ocean sites; the dilatation axes imply frontogenesis at Sites J and K, and frontolysis at Site L. However, the temperature gradient of the surface air over the ocean is very small at this time, thus decreasing the frontogenetical effect of horizontal deformation by the observed wind.

The surface horizontal divergence field analyzed in Figure 2.9 shows the increase in convergence of the

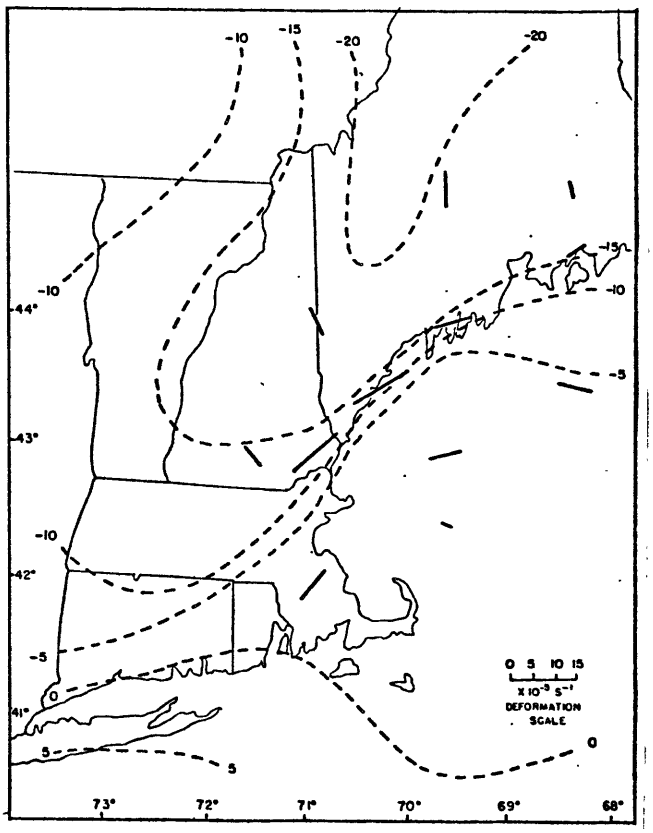

Figure 2.8 Surface isotherms (degrees Celsius) and observed horizontal deformation for 1800 GMT 23 January 1982.

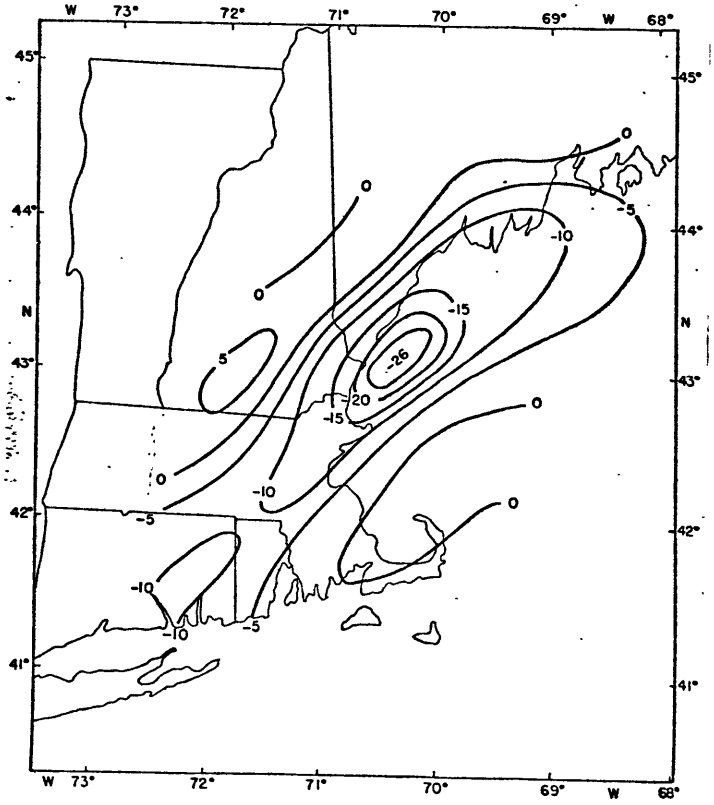

Figure 2.9 Observed horizontal divergence (10^{-5} s^{-1}) for 1800 GMT 23 January 1982.

observed wind along the front, as the magnitude of the relative maximum has more than tripled to a value of $-26 \times 10^{-5} s^{-1}$. The location of this maximum corresponds nicely with the area of heaviest precipitation at this time, illustrating the role of upward motion in inducing intense precipitation. The offshore occurrence of this maximum is in accordance with the previous observation of the wind backing from easterly to northerly at Wood Island indicating a seaward shift of the frontal zone.

The coastal front strengthens to its maximum intensity between 2100 GMT and 0000 GMT. The surface conditions at 0000 GMT 24 January are plotted in Figure 2.10. The map shows that the coastal low is now located in southeastern Connecticut with a central pressure of 998 mb; the central pressure of the system has continued to fall at the steady rate of 5 mb per 3 hours. The coastal front remains most intense along the southern Maine coastline, where remarkably contrasting surface observations across the frontal zone are being reported. Portland, Maine (PWM) is reporting a temperature of $-14^{\circ}C$ with a north-northwesterly wind at 5 m/s while Wood Island, just 21 km away, shows a 1° C temperature with wind out of the southeast at 8 m/s. The same 15° C temperature contrast is being reported between Brunswick, Maine (NHZ) and Seguin Island. Perhaps even more remarkable is the backing to northerly of the light

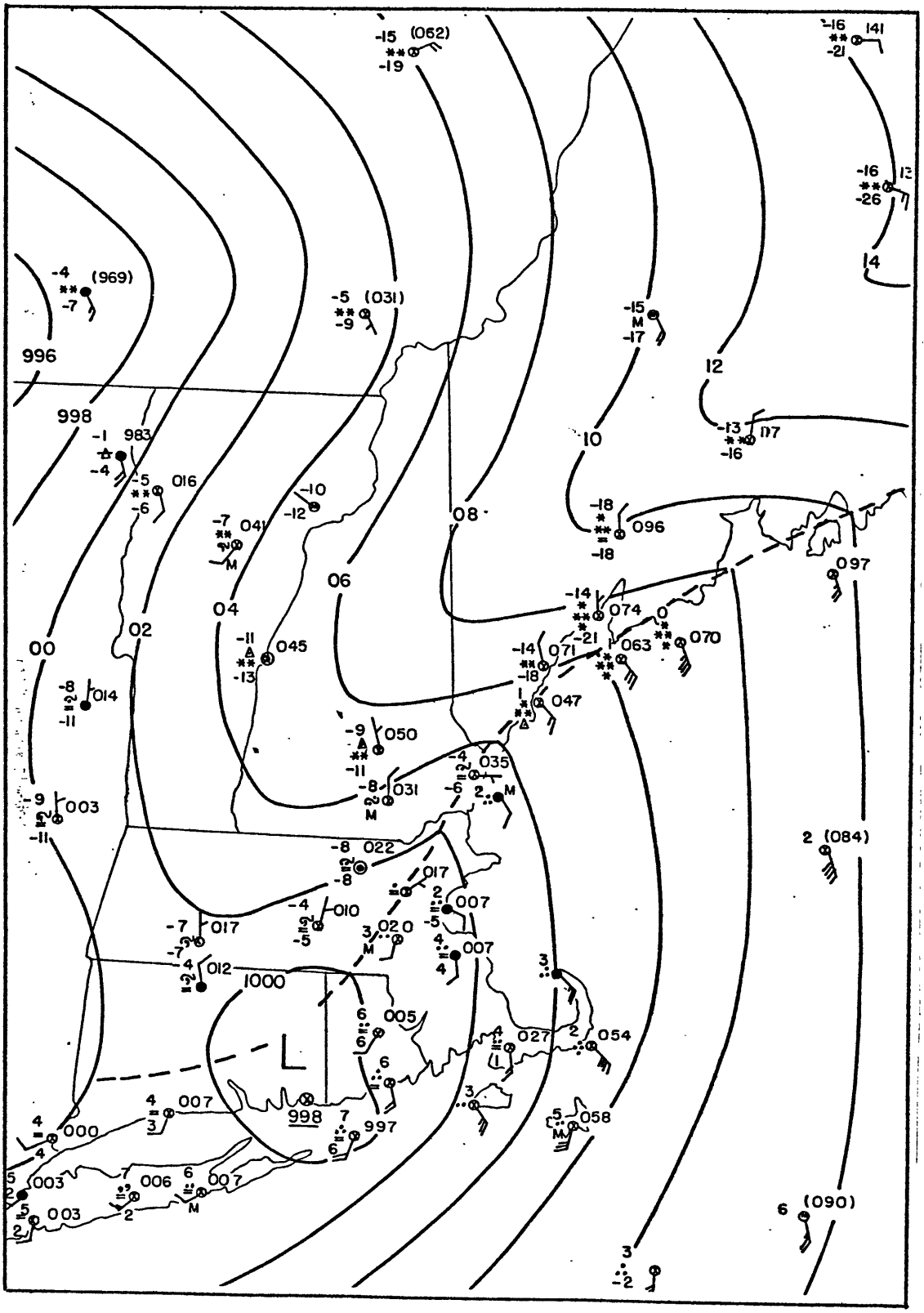

Figure 2.10 Surface analysis for 0000 GMT 24 January 1982.

wind at Brunswick, while nearby Seguin Island is reporting a sustained wind of 15 m/s out of the southeast. The deepening of the cyclone has resulted in strong southeasterly winds over much of the area on the warm side of the front, with maximum sustained winds of 20 m/s being reported at Chatham and Buoy 443. The wind on the cold side of the front maintains its northerly component with slight backing reported at some stations.

By 0000 GMT the location of the coastal front more clearly marks the boundary between frozen and non-frozen precipitation. Snow, freezing rain and drizzle, and ice pellets are now falling on the cold side of the front, while the precipitation on the warm side is mostly rain and drizzle. The exception is along the Maine coast where the coast guard stations continue to report moderate to heavy snow, but with temperatures near the freezing mark and a strong southeasterly flow a changeover to unfrozen precipitation is surely imminent.

The surface isotherms in Figure 2.11 illustrate the sharpness of the temperature gradient along the Maine coastline. They also indicate that the cold air banked inland shows evidence of cutting off into a cold pool in southern Maine. Notice also the relative weakness of the surface temperature gradient in Connecticut after the passage of the deepening cyclone. The temperature gradient over the ocean remains weak at this time.

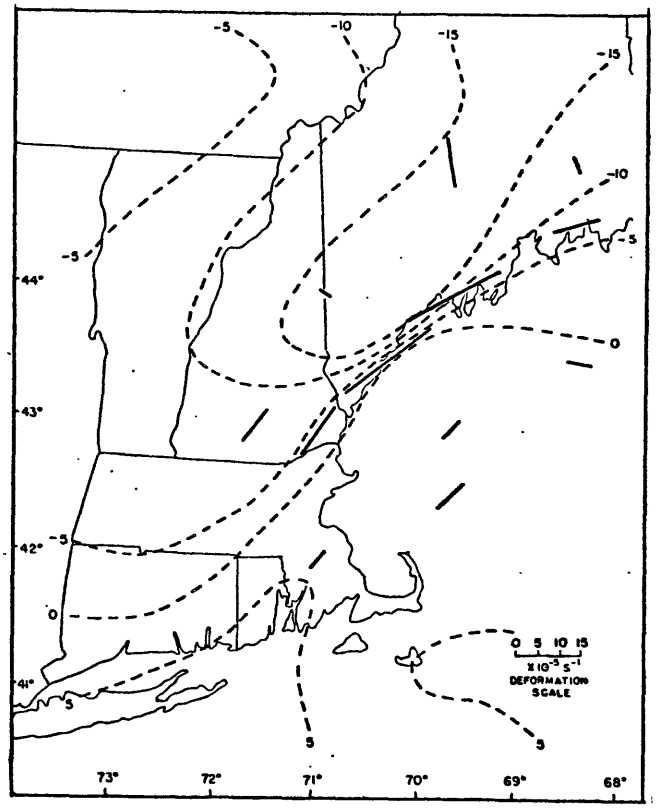

Figure 2.11 Surface isotherms (degrees Celsius) and observed horizontal deformation for 0000 23 January 1982.

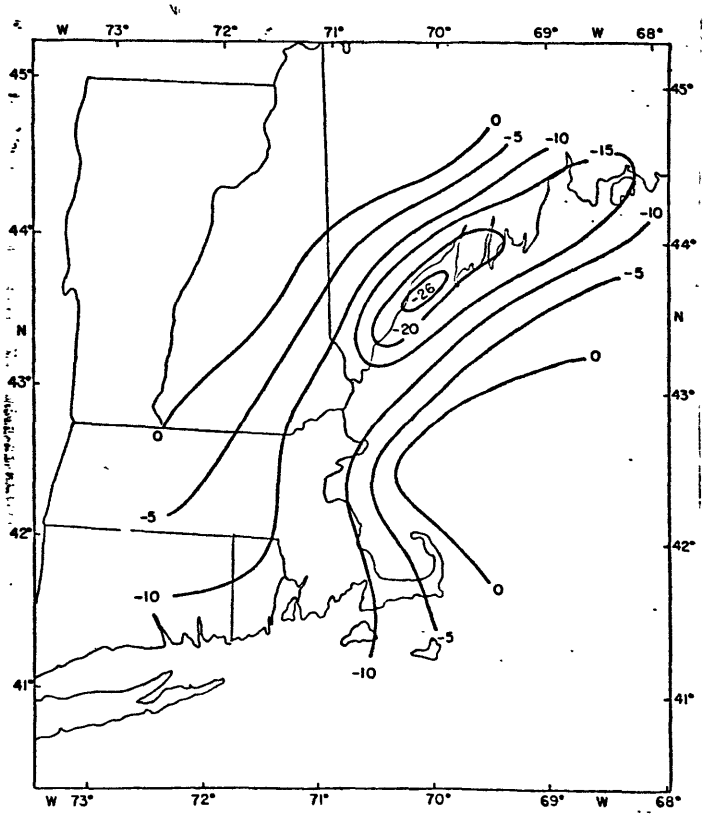

Figure 2.12 Observed horizontal divergence (10^{-5} s^{-1}) for 0000 GMT 24 January 1982.

The frontogenetical effect of the horizontal deformation by the observed wind is remarkable within the strong frontal zone. Deformation magnitudes approach an impressive 30 x 10^{-5} s^{-1} by this time. The significance of these large magnitudes is amplified by the orientation of the dilatation axes; note the small angle they form with respect to the surface isotherms. In fact, the dilatation axis at Site G appears to be parallel to the isotherms, implying the deformation by the observed wind is working in an optimal frontogenetical sense. Meanwhile, the deformation at the inland sites continues to act frontolytically.

The horizontal divergence field shown in Figure 2.12 confirms the intensity of the front in the Portland-Brunswick area, as indicated by the location of the -26 x 10^{-5} s^{-1} convergence maximum. The divergence field looks somewhat different than it did six hours previously, as the convergence center is now located farther north and closer to the coastline. Also, the area of strong convergence is more spread out as evidenced by inspection of the -15 contour which now reaches into the northern length of the Maine coastline.

By 0600 GMT the surface cyclone has progressed northeastward along the coastline and its central pressure has dropped to 990 mb (Figure 2.13). The path of the low

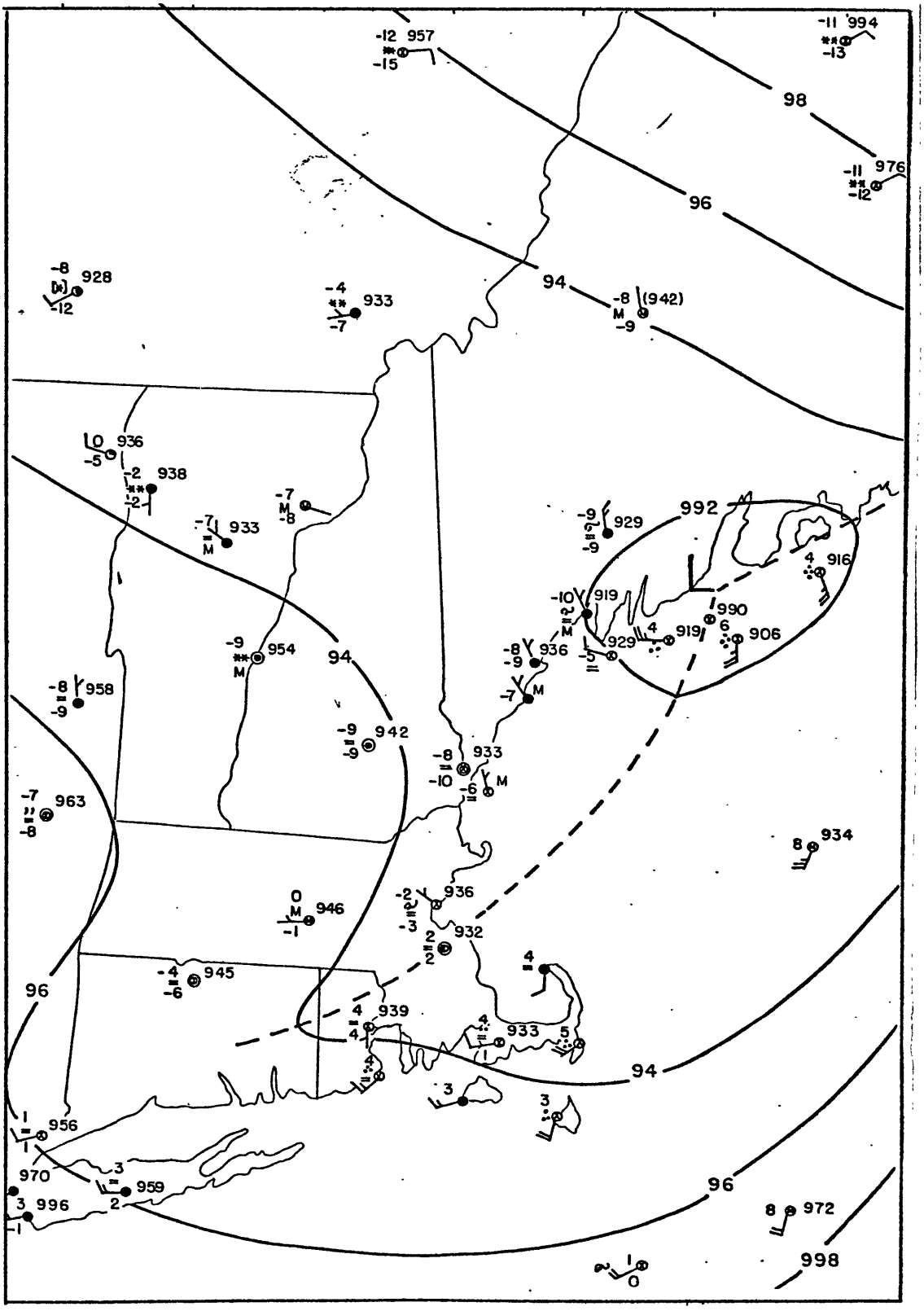

Figure 2.13 Surface analysis for 0600 GMT 24 January 1982.

center along the surface isotherms suggests a tendency for the system to feed on the baroclinicity of the frontal zone. The passage of the cyclone has resulted in the displacement of the front from the Maine coastline; the frontal zone is now more transient and moves offshore as it becomes enveloped by the flow behind the passing low center. The winds behind the low, both inland and offshore, have shifted to northwesterly and westerly. The coastal front ahead of the surface cyclone is still clearly discernible, but its length and intensity have diminished. Admittedly, the surface observations ahead of the low at this time are fewer than before, but supplemental data not shown here imply the diminished strength of the front in advance of the low.

Notice that the passage of the low results in a rapid tapering off of the intensity of precipitation. Moderate rain continues to fall at Manana Island, but precipitation elsewhere behind the cyclone is limited to light freezing rain and drizzle. The expected backing of the wind is observed at most locations. Wind speeds behind the cyclone have diminished as the result of the weaker pressure gradient. In fact, some locations are now reporting calm air (PWM, CON, LEB). Fog is also observed at many stations.

Figure 2.14 illustrates the weakening of the temperature gradient as the frontal zone moves offshore. As suspected, a cold pool of air has cut off in western

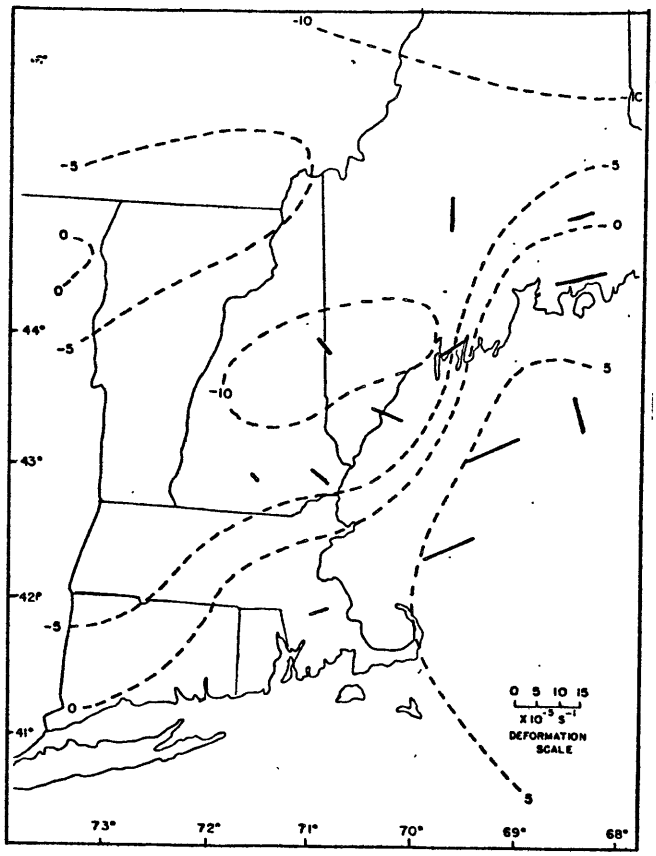

Figure 2.14 Surface isotherms (degrees Celsius) and observed horizontal deformation for 0600 GMT 24 January 1982.

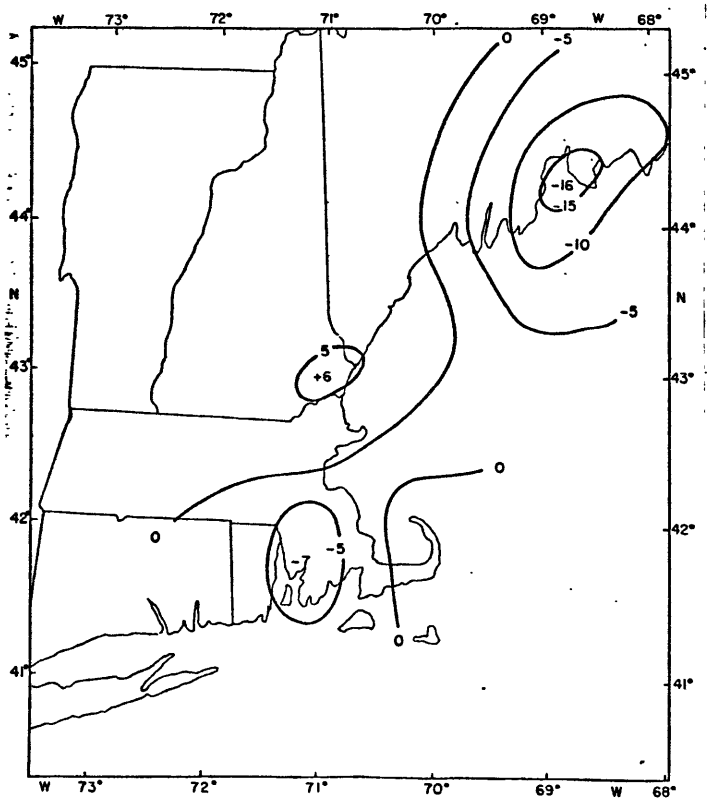

Figure 2.15 Observed horizontal divergence (10^{-5} s^{-1}) for 0600 GMT 24 January 1982.

Maine and eastern New Hampshire as evidenced by the -10^{o} C isotherm. The observed deformation along the coastline has decreased drastically in magnitude and is now acting frontolytically, except ahead of the cyclone at Site E. The magnitude of deformation at the ocean sites has increased considerably as the front moves offshore, but the orientation of the dilatation axes indicates the deformative effect at these site is frontogenetically neutral.

The horizontal divergence field (Figure 2.15) reveals that the relative maximum of convergence has dropped to $-16 \times 10^{-5} s^{-1}$ and is now found at approximately the same location as the surface cyclone instead of well ahead of it as it had been for the past 18 hours. A secondary convergence maximum is also seen in southeastern New England, and this may be associated with the light to moderate rain that continues to fall on Cape Cod and the nearby islands.

Figures 2.16 and 2.17 give the synoptic view of the eastern United States at 1200 GMT 24 January 1982 after the removal of the front from the New England coast. The cyclone that has travelled up the coastline continues to deepen as it approaches Nova Scotia, and it is beginning to merge with the huge cyclone that was previously situated in the Great Lakes region. The two storms will combine and

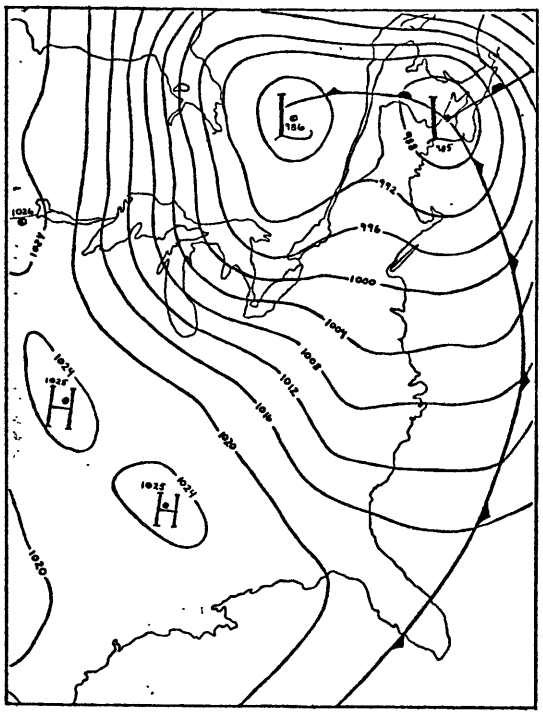

Figure 2.16 Surface pressure and frontal analysis for 1200 GMT 24 January 1982. Isobars labeled in mb.

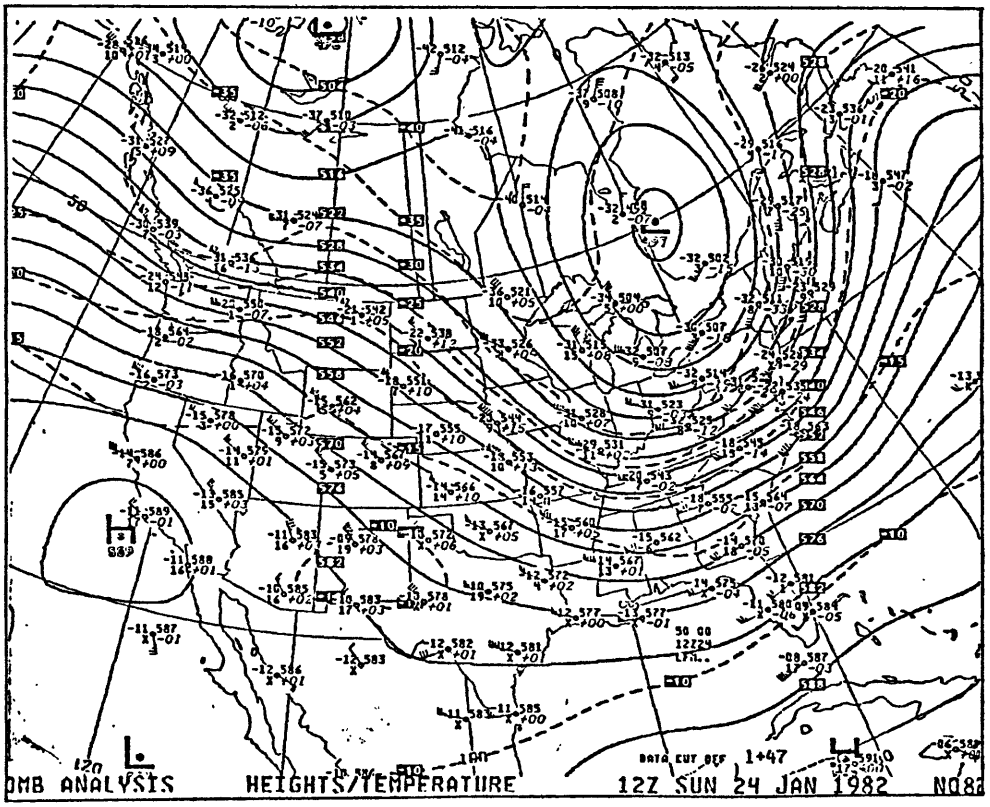

Figure 2.17 500 mb height analysis (dm) for 1200 GMT 24 January 1982. (from NMC)

move north-northwestward with a continuing fall of central pressure. The temperature gradient associated with the coastal front has been enveloped by the northwesterly flow behind the surface low and is now seen as a transient cold front that is well offshore and moving eastward.

We may now examine the field of geostrophic deformation associated with the case of 23-24 January 1982. It is apparent that geostrophic deformation does not play a primary role in coastal frontogenesis forced by onshore flow from a cold anticyclone. Bosart (1975) explains that the maximum horizontal geostrophic deformation is more closely related to the inland pressure ridge rather than the initiation of a frontal zone along the coast, as he illustrates in his documentation of the case of 23-24 December 1970. A similar observation is made in the case just examined. This can be seen in Figure 2.18 which is an analysis of the horizontal geostrophic deformation field at 1200 GMT 23 January, during the initiation of the coastal front in New England. Calculations were made using finite differencing oriented east-west and north-south across a one degree latitude distance. Inspection of the figure shows the maximum occurs well to the southwest of New England in eastern Pennsylvania, and the deformation magnitude tapers off toward the coast. The smallest values are found in the coastal area of New England where

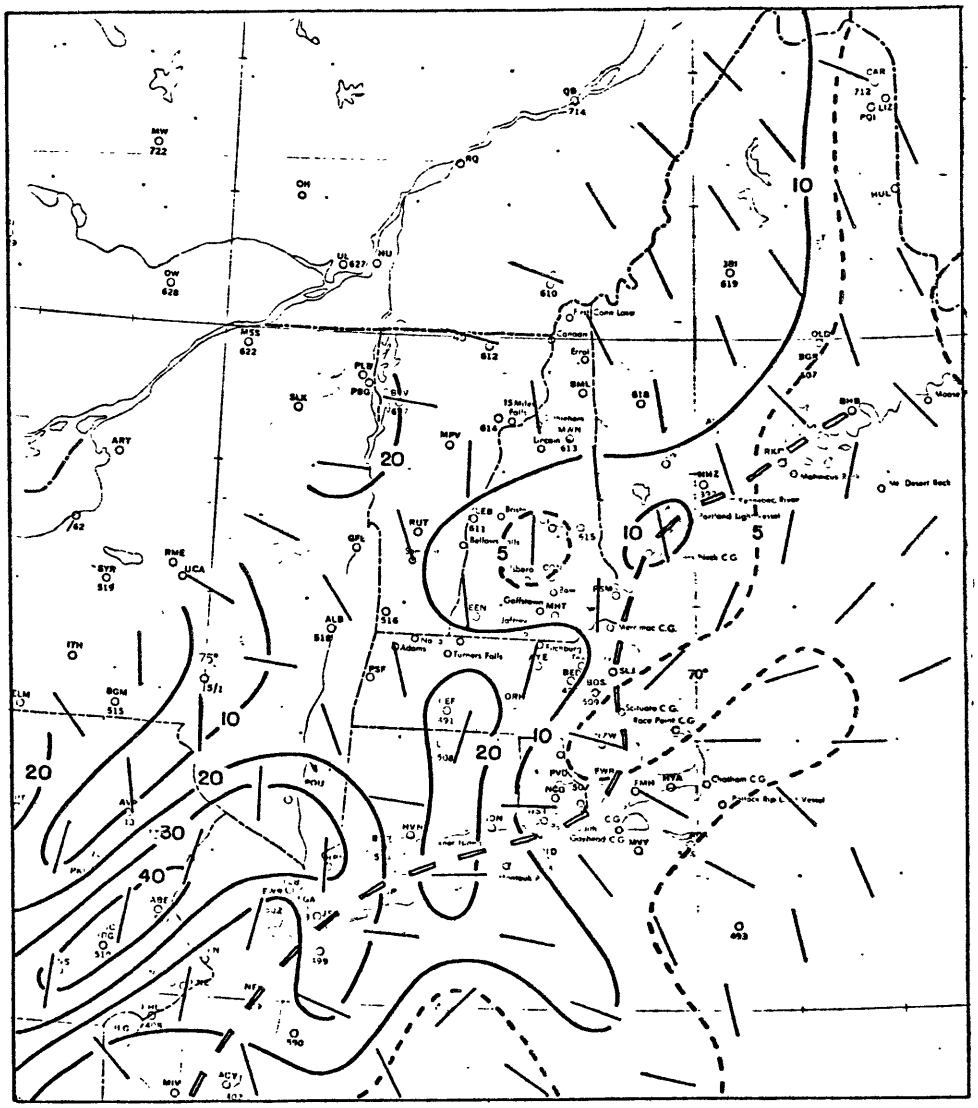

Figure 2.18 Horizontal geostrophic deformation (10^{-5} s^{-1}) for 1200 GMT 23 January 1982. Straight solid lines indicate dilatation axes. Dashed line indicates location of coastal front. Values obtained using one degree latitude grid.

frontogenesis has already begun. Observe how the dilatation axes along the Maine coastline lay normal to the coast indicating a frontolytical effect. This example supports Bosart's observation, as horizontal geostrophic deformation, in both magnitude and direction, is clealy not responsible for the establishment of the coastal front in New England.

Figures 2.19 and 2.20 show the horizontal deformation fields at 1800 GMT and 0000 GMT respectively. Notice how the deformation maximum remains inland throughout the time series. At 1800 GMT, a relative minimum occurs along the coastline where the front is most pronounced at this time. The dilatation axes indicate a weak frontolytical effect in the Portsmouth (PSM) and Portland (PWM) areas, and a weak frontogenetical effect in the Brunswick (NHZ) area. By 0000 GMT the effect of geostrophic deformation becomes frontolytical near Brunswick, and this is also the location of a relative minimum of deformation magnitude.

These observations support the theory that horizontal geostrophic deformation does not play an important role in the initiation and development of a coastal front associated with a cold anticyclone. Further investigation, however, has led to the speculation that there is another type of coastal front forcing that does show some relevance to the synoptic scale geostrophic deformation associated with a weak, migrating cyclone. This mechanism will be

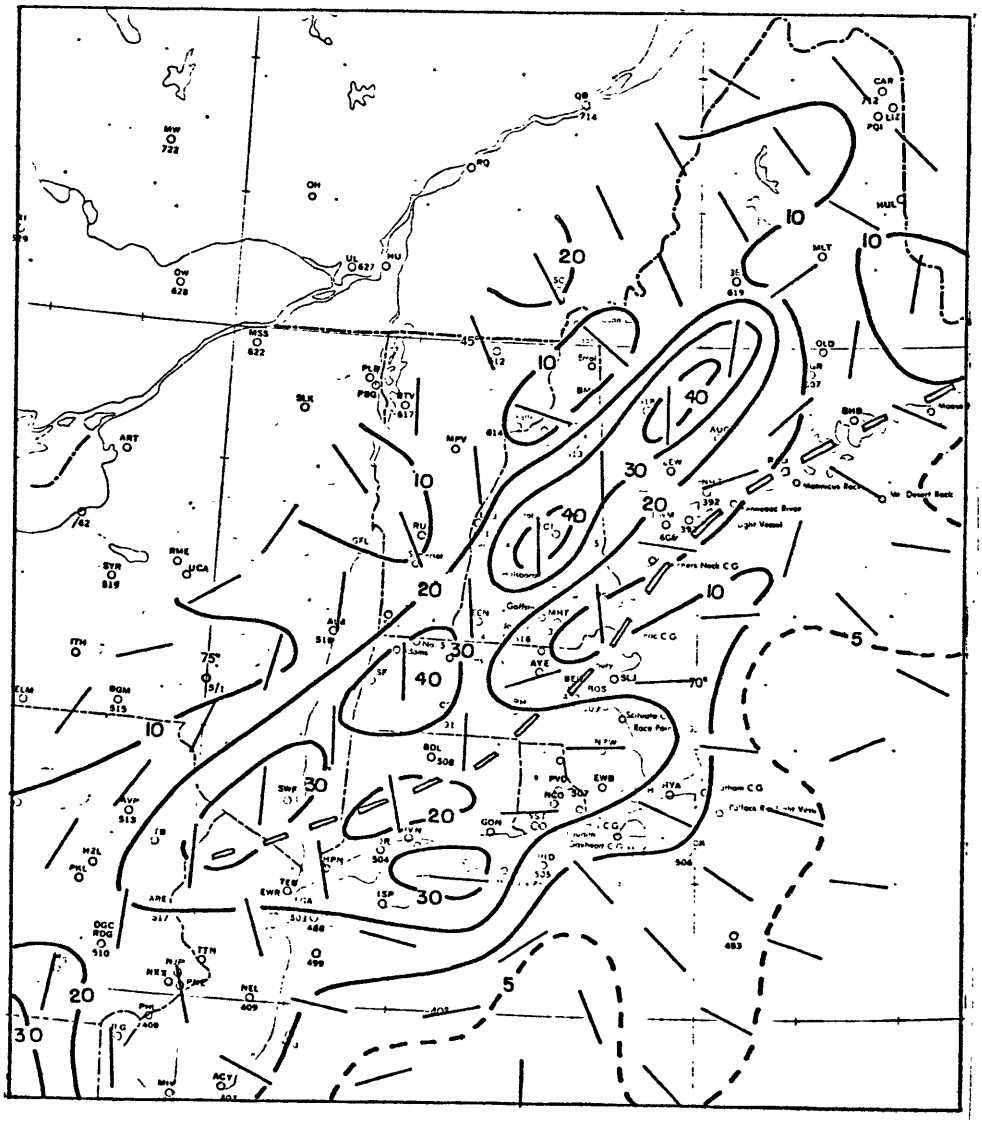

Figure 2.19 Horizontal geostrophic deformation (10^{-5} s^{-1}) for 1800 GMT 23 January 1982.

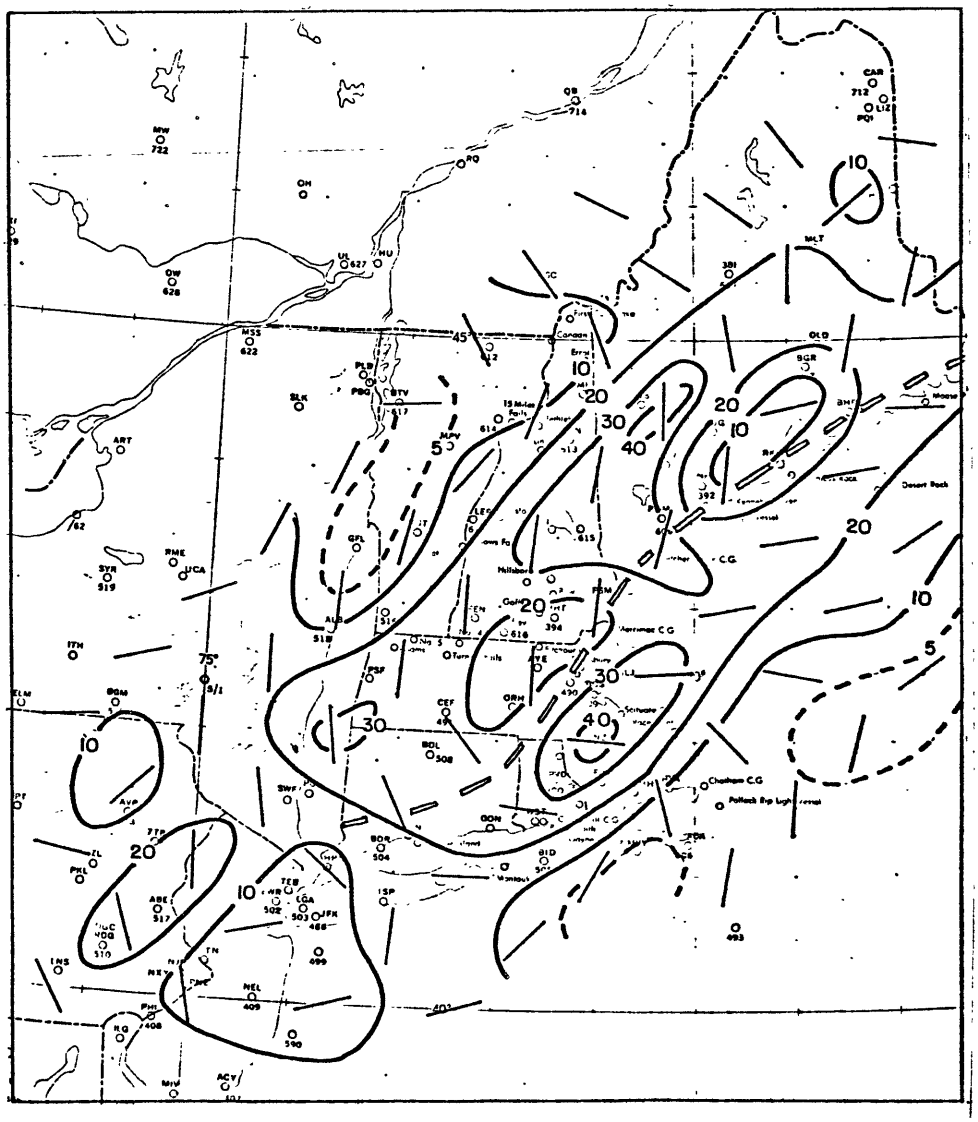

Figure 2.20 Horizontal geostrophic deformation (10^{-5} s^{-1}) for 0000 GMT 24 January 1982.

considered in detail in the next chapter.

As a final view of the case of 23-24 January 1981, it will be useful to consider some suporting data that will help to exemplify the characteristics of a New England coastal front initiated by geostrophically onshore flow from a cold anticyclone. Figure 2.21 is a temperature sounding for Portland that illustrates the shallowness of the front. The sounding was taken at 0000 GMT 24 January 1982 when the front was near peak intensity in this area. It shows a shallow isothermal layer from 1008 mb (surface) to 1000 mb, and then a sharp inversion to 972 mb where the temperature increases to -2° C. The coastal front phenomenon in this case is a frontal structure that reaches less than half a kilometer up into the atmosphere. Notice the strong shear in the wind from the the surface to 850 mb that reflects the extreme baroclinicity; a 5 m/s north wind at the surface veers 180 degrees to a 30 m/s southerly wind at 850 mb.

Figure 2.22 is a product of the 1981-82 New England Storms Project research performed at M.I.T. The data was obtained by recording surface observations while traversing the front by automobile in northeastern Massachusetts on 23 January. The graph is a plot of temperature-vs.-distance normal to the front, and it rather spectacularly illustrates the strength of the boundary layer temperature

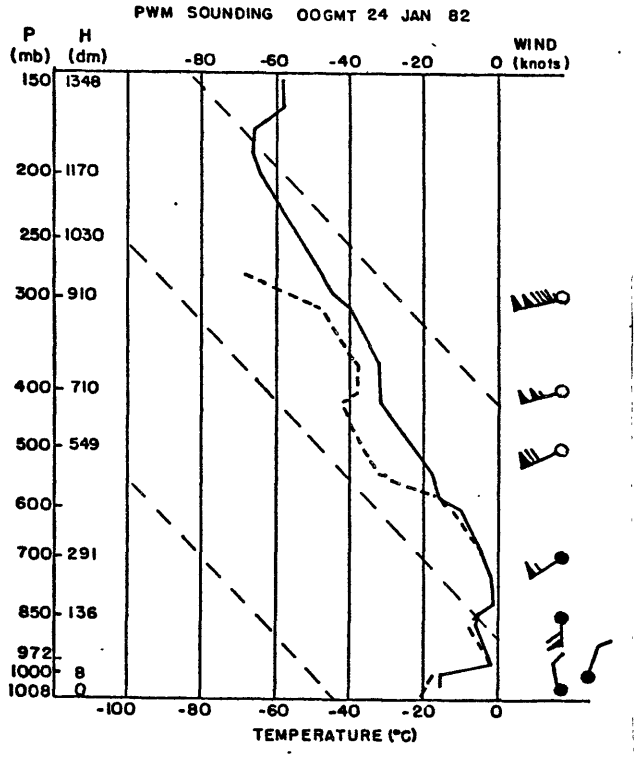

Figure 2.21 Temperature sounding from Portland for 0000 GMT 24 January 1982.

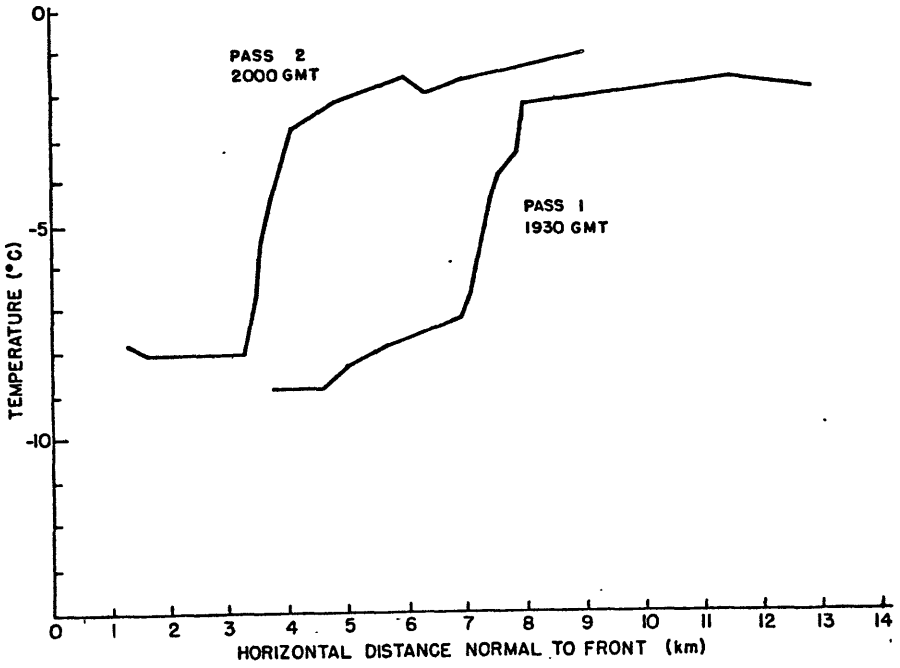

Figure 2.22 Surface temperature profile from northeastern Massachusetts for 23 January 1982.

gradient. It reveals horizontal temperature contrasts of more than 5°C over a distance of less than a kilometer, which is an example of one of the more extreme horizontal temperature gradients found in the earth's atmosphere. Additional horizontal temperature gradient measurements for this case are provided in the appendix, as well as calculations of frontogenesis rates.

Figure 2.23 is an analysis of the 24-hour precipitation totals ending 1200 GMT 24 January. It shows a relative maximum of more than 30 mm of precipitation in the vicinity of Portland where the most intense portion of the coastal front occurred, and it certainly lends credence to the speculation that the presence of a coastal front will enhance local precipitation amounts. Notice that a relatively light amount of precipitation fell in eastern Massachusetts between Boston (BOS) and Providence (PVD), as well as on Cape Cod. An inspection of the isotherm maps shows that this was also an area where the horizontal temperature gradient was consistently a relative minimum. A second precipitation maximum is seen in western Long Island, and this can also be correlated to the strong gradient of temperature that was present in this area.

Figure 2.24 shows 3-hourly time series of two pairs of stations which concisely illustrate the contrasting surface weather conditions across the frontal zone. The severity of the front is appreciated when considering that the

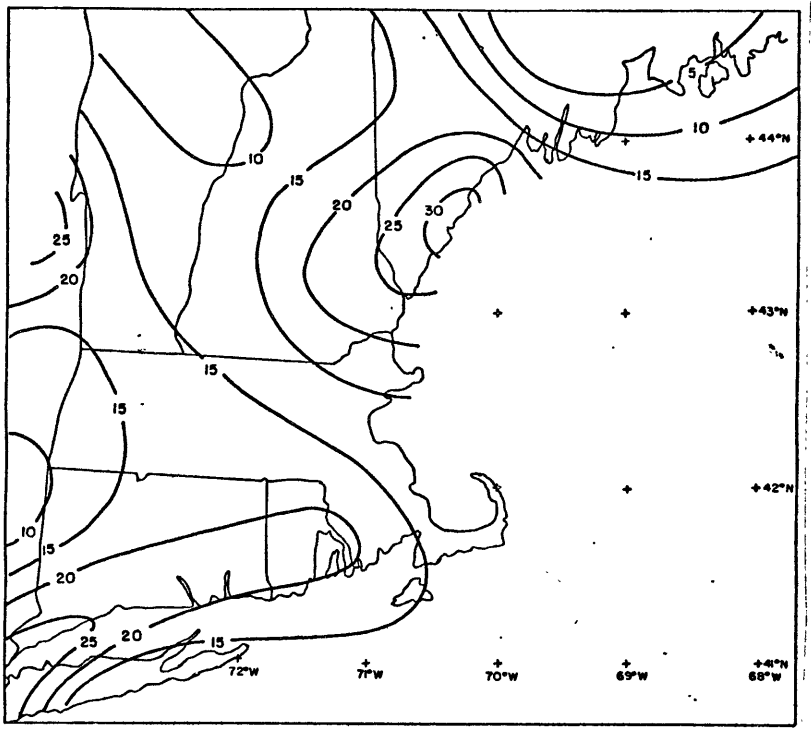

Figure 2.23 24-hour precipitation totals (mm) ending 1200 GMT 24 January 1982.

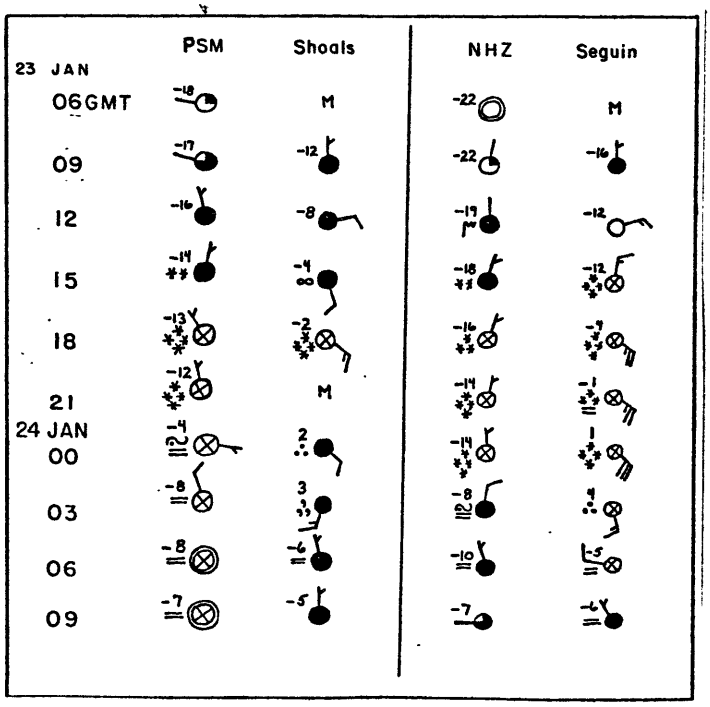

Figure 2.24 3-hourly station observations at Portsmouth (PSM), Isles of Shoals, Brunswick (NHZ), and Seguin Island. Temperatures in degrees Celsius. One full wind barb = 10 knots (approximately 5 m/s).

distance between PSM and the Isles of Shoals is only 20 km, and the distance between NHZ and Seguin Island is less than 30 km. The PSM-Shoals time series shows a veering of wind at PSM between 1200 GMT and 1500 GMT, while a backing to northwesterly occurs during the next three hours. This type of wind behavior is typical on the cold side of a coastal front. Ballentine (1980) claims that the backing of the wind on the cold side of the front is an indirect response to the release of heat fluxes from the ocean. He explains that heat from the ocean diffuses upward through the boundary layer resulting in greater pressure falls over the ocean than over land. The wind over land responds to this isallobaric effect by flowing in the direction of most rapidly falling pressure. Such an effect, however, is not apparent in the case of 23-24 January as uniform pressure falls occur over the entire New England region, including the area over the ocean.

Another note of interest found in the PSM time series illustrates the forecasting challenge in the vicinity of a coastal front. As the front creeps inland between 2100 GMT and 0000 GMT, the wind at Portsmouth shifts from offshore to onshore and the result is a dramatic change in weather conditions. Inspection of the hourly reports reveals that between 2200 GMT and 2300 GMT the temperature at PSM jumps from $-11^{\circ}C$ to $-1^{\circ}C$, a remarkable $10^{\circ}C$ increase in just one hour. The temperature jump is accompanied by a change from

heavy snow to a mixture of ice pellets, freezing rain, and light snow. Portsmouth's stay in the warmer air is short-lived; three hours later they are back into northwesterly flow and the temperature plummets down to -9° C. Such dramatic behavior in surface weather conditions exemplifies the difficulty in local forecasting produced by the presence of such an intense boundary layer phenomenon.

3.0 Frontogenesis Initiated By A Zipper Low: Case of 15 December 1981

The observations presented thus far have supported the theory that coastal frontogenesis associated with a cold anticyclone cannot be initiated by horizontal geostrophic deformation. Further investigation, however, has led to the speculation that there is another type of coastal front forcing that appears to be related to the synoptic scale geostrophic deformation associated with a zipper low. As described earlier, the zipper low has the effect of "pinching" the isotherms in the vicinity of the cyclone, thus producing a local strengthening of the horizontal gradient of temperature. This effect is illustrated in the following case of 15 December 1981. For the reader's reference, the locations of the main observing stations used in this case are shown in Figure 3.1.

The surface analysis for 0000 GMT December 1981 is provided in Figure 3.2. It is at this time that we first see the closed circulation of the zipper low, which appears on this map as a 1011 mb cyclone located in North Carolina. The cyclone is a small pulse that has emerged from a larger system located in the Gulf of Mexico. The entire eastern portion of the country is cloudy at this time, while light rain and snow is falling over a large area. A surface front lies ahead of the cyclone where an 8 to 12 $^{\circ}$ C

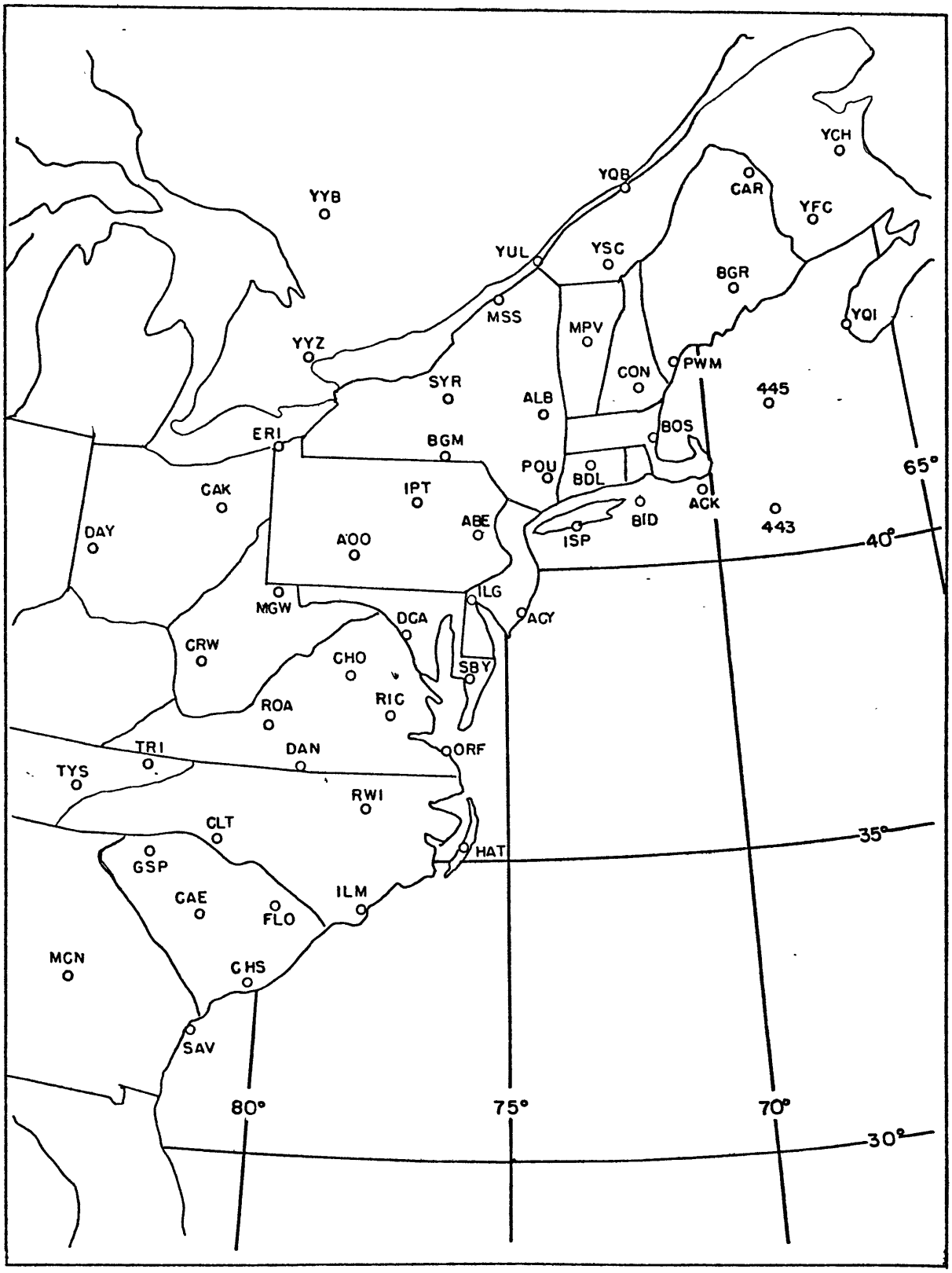

Figure 3.1 Locations of key observing stations in eastern United States and Canada.

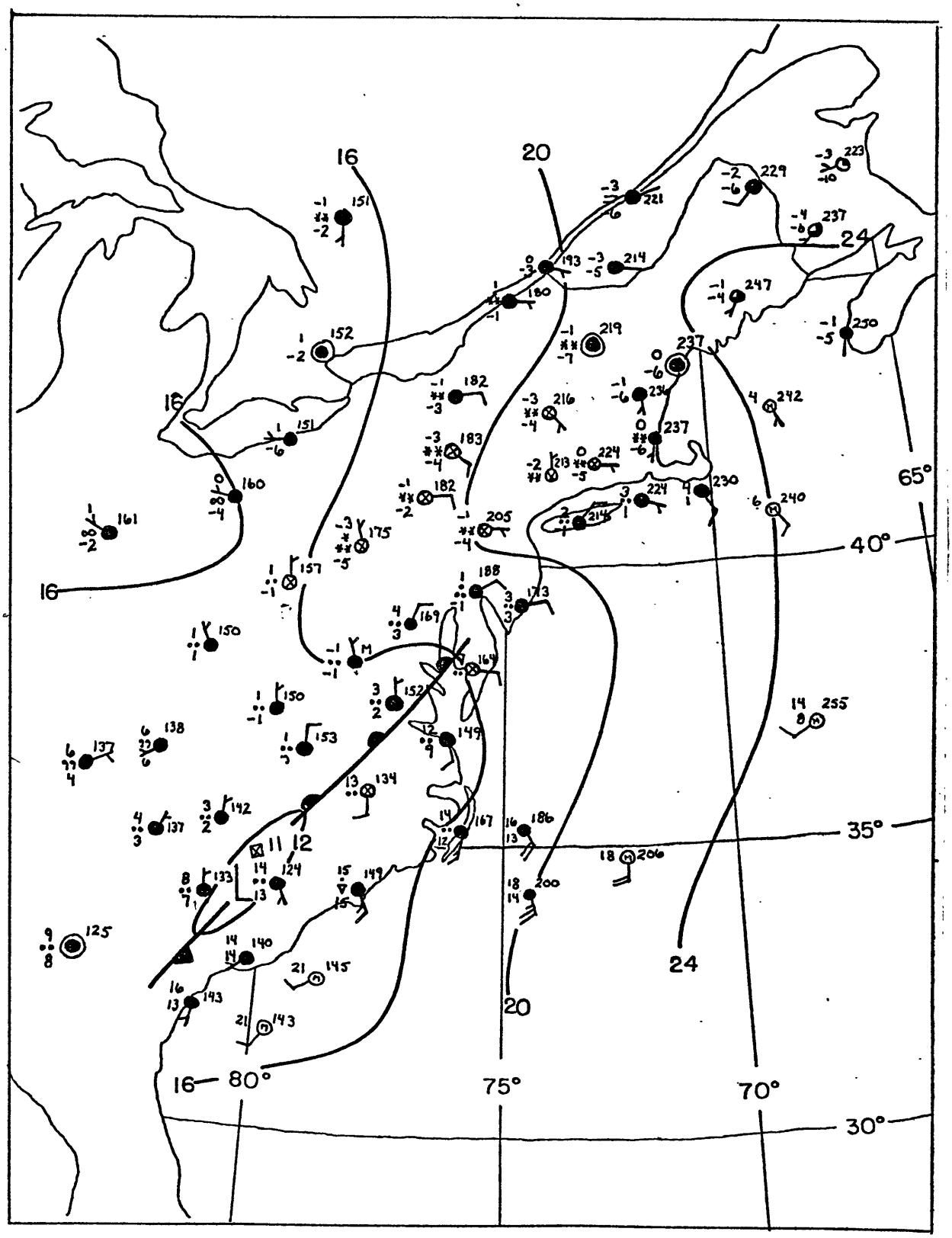

Figure 3.2 Surface analysis for 0000 GMT 15 December 1981. Pressure in mb, temperature and dew point in degrees Celsius. One full wind barb = 10 knots (approximately 5 m/s).

temperature contrast is observed across the frontal zone. Notice how the geostrophic flow runs parallel to the coast in the area of the frontal zone. Accordingly, the observed wind on either side of the front has a larger component parallel to the front than was observed in the cold anticyclone case of 23-24 January.

The frontal zone can be seen in the isotherms drawn in Figure 3.3. The location of the low pressure center is denoted on this map by an "X" enclosed within a square. The temperature gradient is strong ahead of the surface cyclone until it weakens abruptly in the Chesapeake Bay area where the "pinch" in the isotherms ends. It is this pinching effect that is presumably associated with the small surface low.

The horizontal geostrophic deformation field at 0000 GMT is analyzed in Figure 3.4. The field is fairly flat at this time; there is a relative maximum along the coast to the east of the low. The dilation axes within this area of maximum deformation are aligned normal to the coastline and the surface isotherms, indicating a frontolytical effect. More important at this time is the area ahead and to the left of the surface cyclone, where the dilatation axes are parallel to the surface isotherms. The zipping of the isotherms is taking place here. The pinching effect coincides nicely with this area of frontogenetical geostrophic deformation.

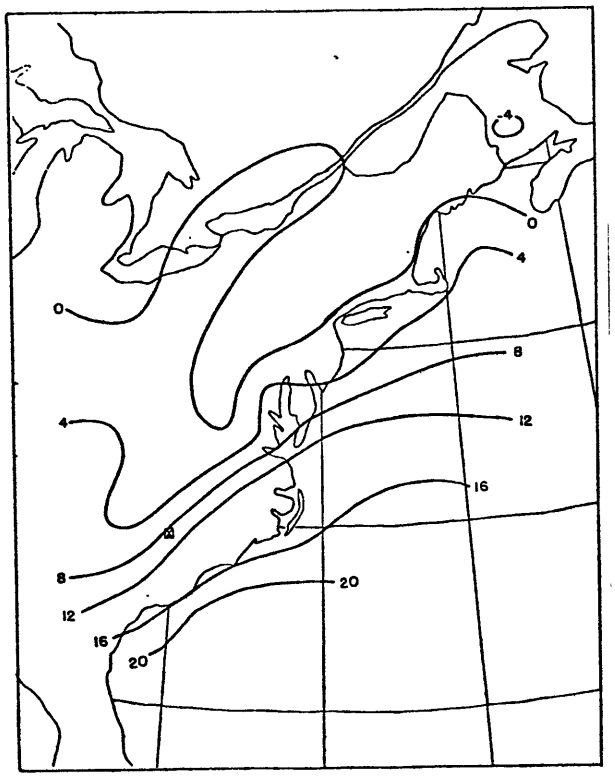

Figure 3.3 Surface isotherms (degrees Celsius) for 0000 GMT 15 December 1981. "X" enclosed within square indicates location of surface cyclone.

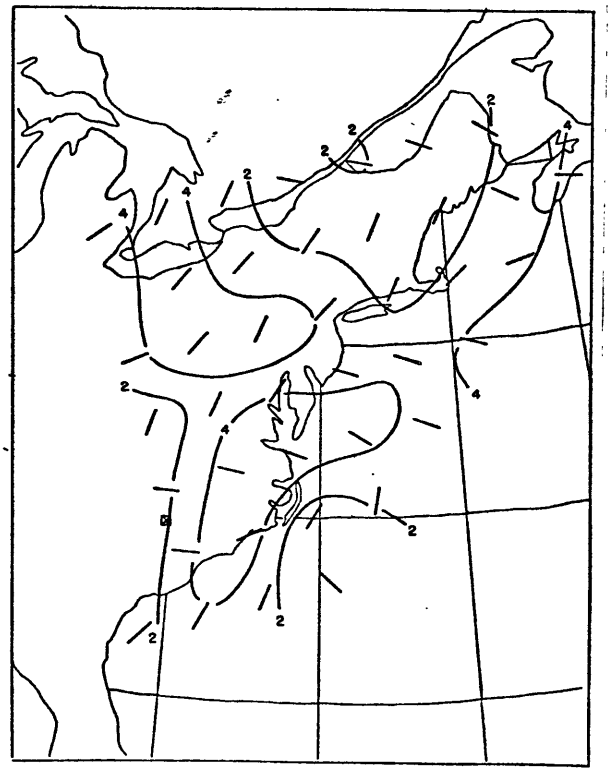

Figure 3.4 Horizontal geostrophic deformation (10^{-5} s^{-1}) for 0000 GMT 15 December 1981. Solid straight lines indicate axes of dilatation. Calculations made using 300 km grid size.

By 0600 GMT the low center has moved rapidly northeastward and is now situated to the south of the New Jersey coast (Figure 3.5). The central pressure of the system has dropped to 1007 mb, a decrease of 4 mb over the past six hours. The frontal zone ahead of the low now reaches into the ocean area off the Maine coast. The front behind the low has maintained its identity and is seen as the cold front running southward to southern Georgia. The precipitation remains widespread and light, and has perhaps become somewhat more spotty. The only report of moderate rain is at Atlantic City, New Jersey (ACY) which is very near the low center at this time.

Figure 3.6 shows that the northeastward progression of the surface cyclone appears to have had the effect of zipping up the thermal gradient, as the strongest temperature gradient occurs in the vicinity of the low. This effect is best illustrated by the pinching of the 16°C isotherm just to the south of the cyclone. Ahead of the cyclone the temperature gradient tapers off considerably.

The geostrophic deformation field (Figure 3.7) shows a relative minimum centered at nearly the exact location of the zipper low. We do see once again, however, the appearance of a frontogenetically favorable geostrophic deformation maximum ahead and to the left of the cyclone. The deformation field has taken on a much more clearly defined appearance, with the development of distinct maxima

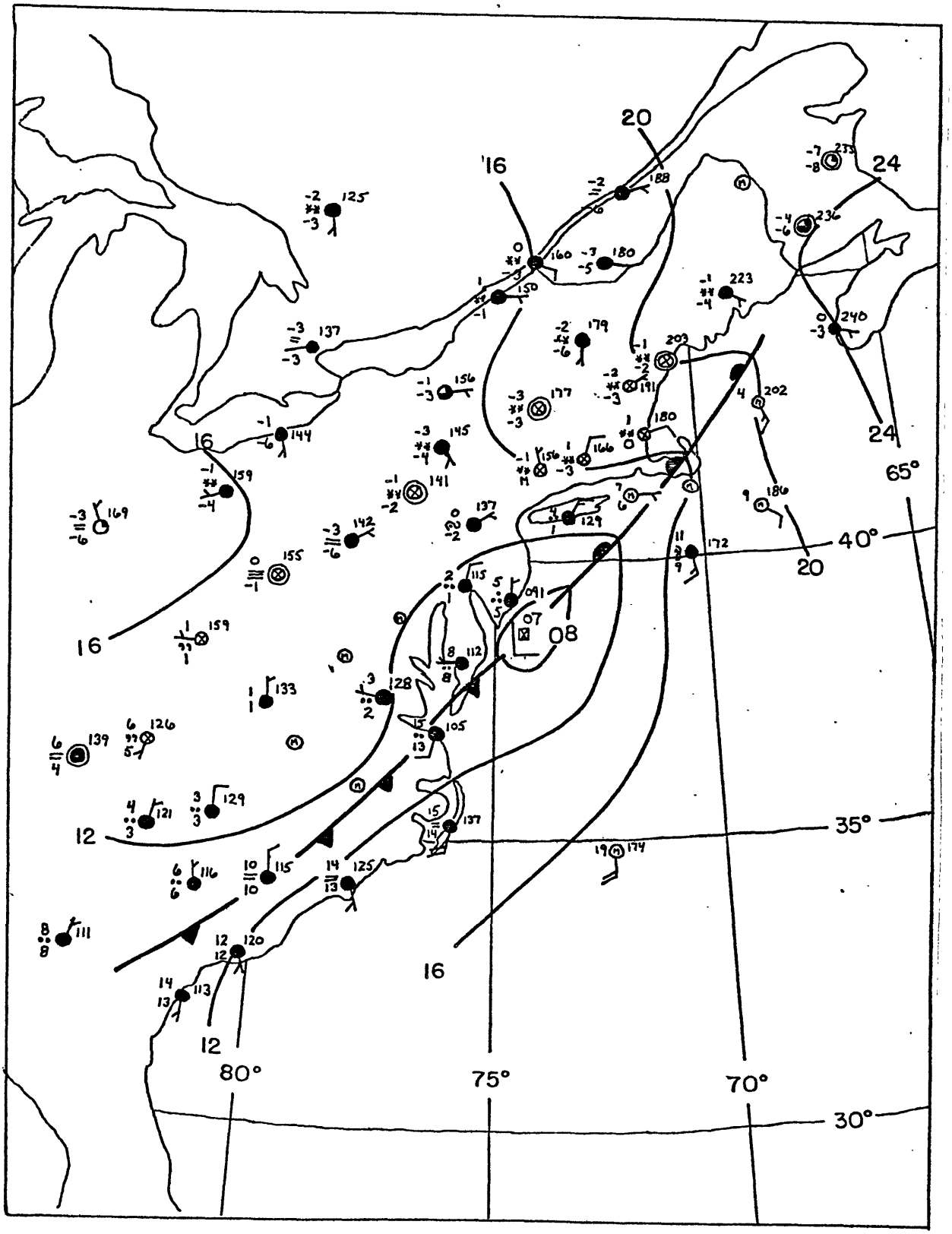

Figure 3.5 Surface analysis for 0600 GMT 15 December 1981.

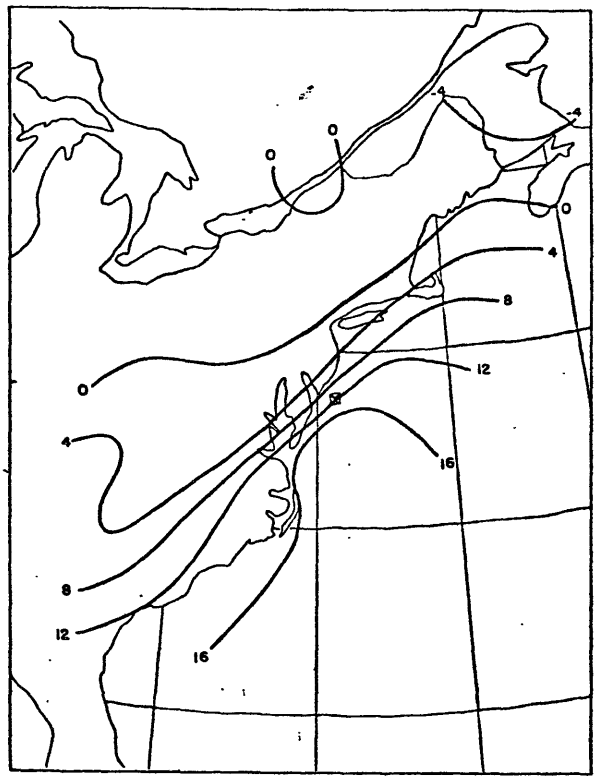

Figure 3.6 Surface isotherms (degrees Celsius) for 0600 GMT 15 December 1981.

Figure 3.7 Horizontal geostrophic deformation (10^{-5} s^{-1}) for 0600 GMT 15 December 1981.

and a minumum; the magnitude of the maximum ahead of the low has incresed considerably to a value of 11 x 10^{-5} s^{-1} by this time. Its appearance suggests a continuation in the zipper effect of the low.

The movement of the zipper low has slowed considerably by 1200 GMT (Figure 3.8); by this time it has advanced only as far as Cape Cod, Massachusetts. The system has retained its elongated shape, and its central pressure has dropped only 1 mb to a value of 1006 mb. The wind over the ocean to the east of the cyclone has increased to 10 to 15 m/s while the wind on the cold side of the front remains northerly at approximately 5 m/s. The frontal zone behind the zipper low continues to maintain its identity offshore, while farther to the south we see the appearance of the low pressure center that has moved northeastward out of the Gulf of Mexico. The precipitation at this time remains light at most observing stations and it appears that there are now two distinct areas of precipitation, one associated with each of the two low pressure systems. Meanwhile, the entire eastern portion of the country remains under overcast skies.

The surface temperature field in Figure 3.9 shows that the pinch in the isotherms has moved northward with the advance of the surface cyclone; it is now located near the eastern side of Long Island, just behind the low pressure

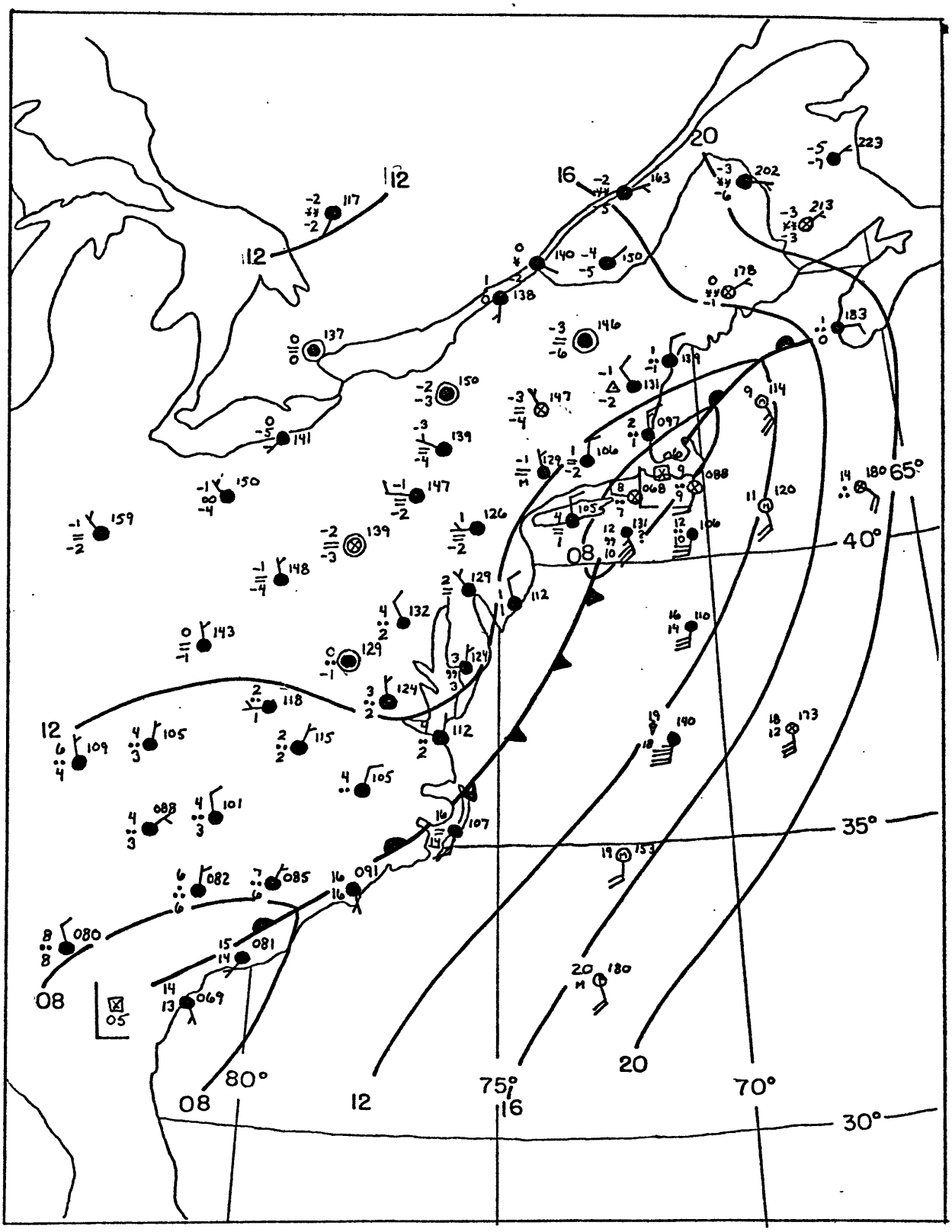

Figure 3.8 Surface analysis for 1200 GMT 15 December 1981.

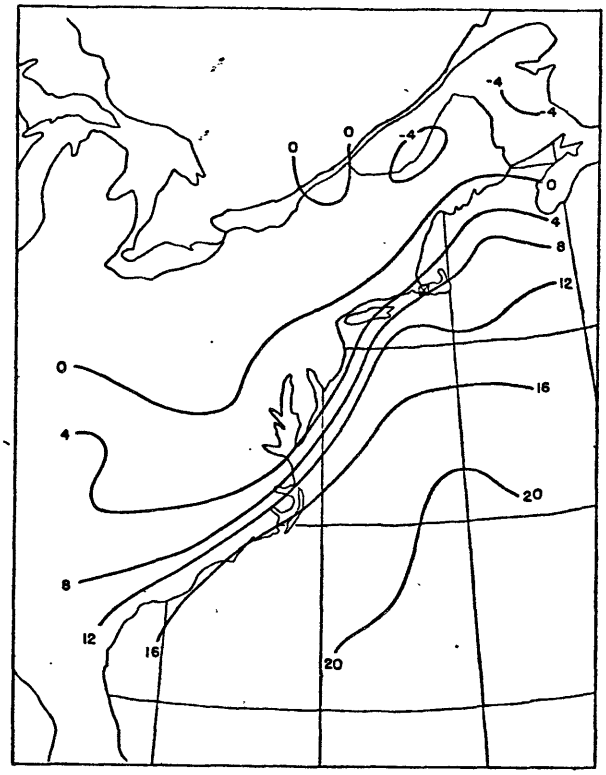

Figure 3.9 Surface isotherms (degrees Celsius) for 1200 GMT 15 December 1981.

Figure 3.10 Horizontal geostrophic deformation (10^{-5} s^{-1}) for 1200 GMT 15 December 1981.

center. The location of the pinch behind the low center may be explained by the cold shallow water to the east of Cape Cod which has the effect of "re-shaping" the surface air isotherms in this area. As mentioned, the frontal zone behind the cyclone remains very well defined as witnessed by the close packing of the isotherms all along the Atlantic coastline. The horizontal deformation field shown in Figure 3.10 reveals the continued presence of the frontogenetically favorable geostrophic deformation maximum ahead and to the left of the zipper low. The central value of this maximum has increased to 13 x $10^{-5} s^{-1}$. Along the Atlantic coastline behind the zipper low the dilatation axes are now oriented frontolytically, indicating that the frontogenetical role that geostrophic deformation played in initiating the frontal zone is apparently not a positive factor in maintaining the frontal zone far behind the cyclone at this time.

By 1800 GMT (Figure 3.11) the zipper low has deepened to 1003 mb and is approaching Nova Scotia. The cyclone by this time has developed a more distinct and intense circulation; the isobars in this figure have been drawn to accomodate the pressure readings from the ships located in the area, but the local wind reports suggest that the storm center could arguably be plotted a bit farther to the east. In any event, the storm has certainly developed a stronger

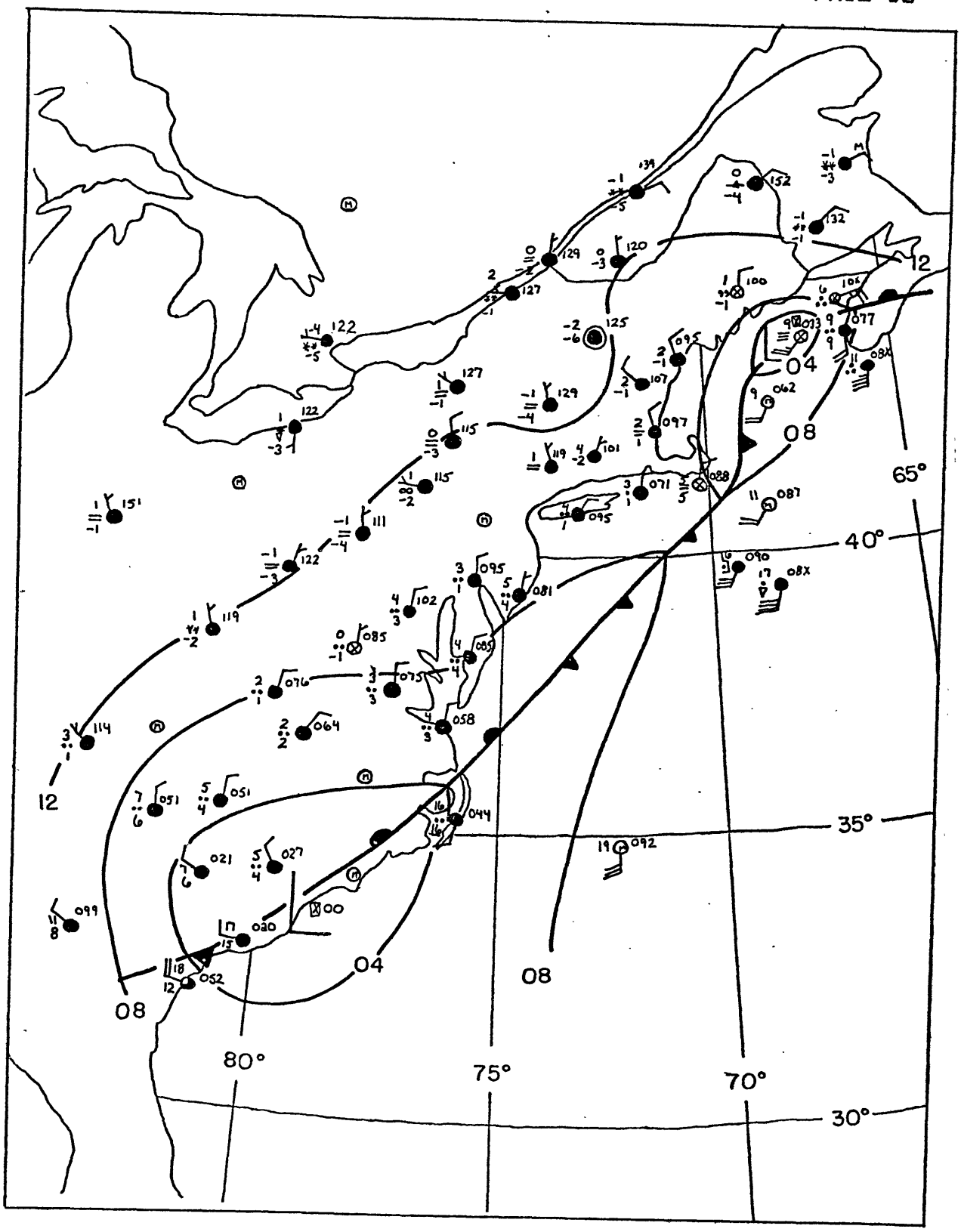

Figure 3.11 Surface analysis for 1800 GMT 15 December 1981.

cyclonic circulation and can no longer be referred to as a weak "pulse". The reports of moderate rain from the local ships indicate that the precipitation ahead of the system may be intensifying, but since we did not have benefit of these particular ship reports six hours earlier, we cannot check the continuity of their precipitation observations. Behind the cyclone, the precipitation has ended abruptly at most stations, unlike the lingering precipitation that was reported behind the cyclone when it was a weak system farther south on the Atlantic coastline. The storm that has moved out of the Gulf of Mexico has now deepened to 1000 mb and is located on the southern North Carolina coast. This system will move northward and combine with the zipper low to form a much stronger cyclone in eastern Canada.

As the zipper low begins to develop into a strong cyclonic system, we can see the final stages of the zipper effect in Figure 3.12. The effect is no longer as dramatic as it had been previously, but it is still evidenced by the pinching of the $0^{\circ}C$ and $8^{\circ}C$ isotherms seen in northeastern Maine. As mentioned, the storm system to the south will race northward along the baroclinic zone that remains on the coastline and combine with the deepening zipper low to form a powerful system in eastern Canada.

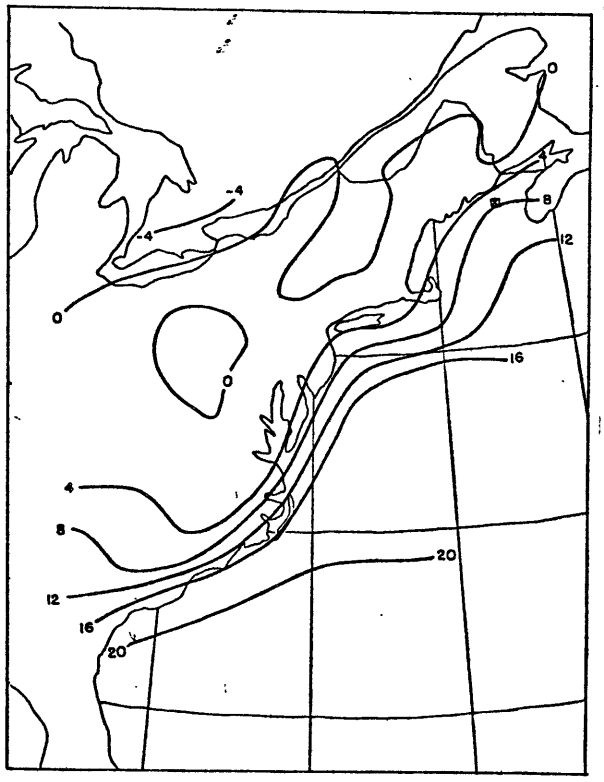

Figure 3.12 Surface isotherms (degrees Celsius) for 1800 GMT 15 December 1981.

4.0 Discussion

In discussing the role of the zipper low in initiating coastal frontogenesis, it should be made clear that the effect of this type of frontogenetical mechanism is by no means restricted to coastal areas. It has been observed that weak cyclones of this type are capable of producing a strengthening of the thermal gradient in regions far removed from the coastline. However, the effect of the zipper low as a frontogenetical mechanism is considered to be most dramatic in areas of pre-existing baroclinicity. Therefore the large land-sea temperature contrast found along the Atlantic coast in late fall and early winter provides an ideal environment for the manifestation of such a process. In light of this, a reasonable comparison may be made between the roles of the zipper low and the cold anticyclone in initiating and maintaining coastal frontogenesis.

The suggestion that frontogenesis may be initiated by horizontal wind deformation fields acting on pre-existing horizontal temperature gradients was first proposed by Bergeron (1928) and has since been supported by analytic models such as those developed by Stone (1966) and Hoskins and Bretherton (1972). It is suggested here that the zipper low's effect of strengthening the horizontal temperature gradient depends upon the frontogenetically favorable deformation field provided by the geostrophic

flow of the system. The zipper low is typically a weak cyclone whose closed geostrophic circulation covers a relatively small area. Ahead of the low center and to its left, the geostrophic circulation "opens up" as evidenced by a diffluence in the surface isobars. A schematic illustration of the typical isobaric pattern associated with a zipper low is shown in Figure 4.1. The dashed lines indicate the approximate orientation of the thermal gradient along the Atlantic coastline with respect to the elongated low. The figure shows how the geostrophic flow ahead of the low slows down in the direction of motion at the exit region of the circulation where the isobars become diffluent. The relative magnitudes of the horizontal geostrophic deformation field for this isobaric pattern are given in Figure 4.2. It shows an area of large deformation magnitude in the vicinity of the low center, which corresponds to the strong confluence and diffluence of the geostrophic flow. A weak region appears slightly to the left of the low center where the horizontal deformation magnitude diminishes to zero, i.e. where the geostrophic flow changes from confluent to diffluent. The relative magnitudes shown on this map must be considered in conjunction with the direction of the axes of dilatation, which is shown in Figure 4.3. This figure was derived from the orientation of the dilatation axes with respect to the dashed lines (isotherms) in Figure 4.1. The

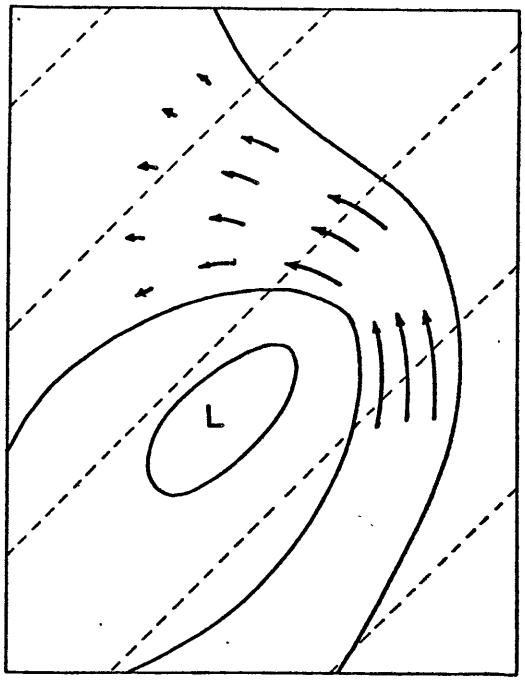

Figure 4.1 Schematic illustration of isobaric pattern (solid lines) associated with zipper low. Dashed lines represent approximate orientation of isotherms.

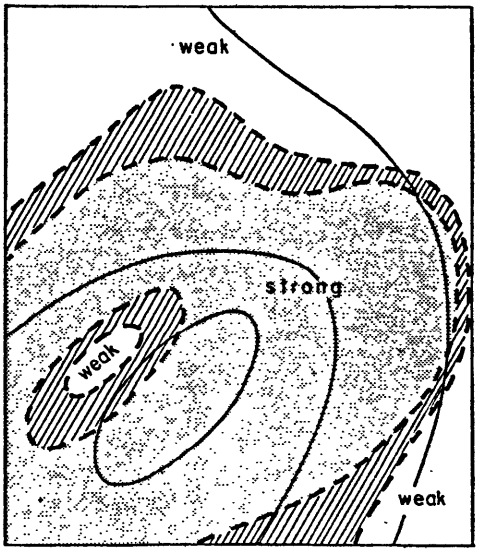

Figure 4.2 Relative magnitude of horizontal geostrophic deformation associated zipper low. (Solid lines represent isobars.)

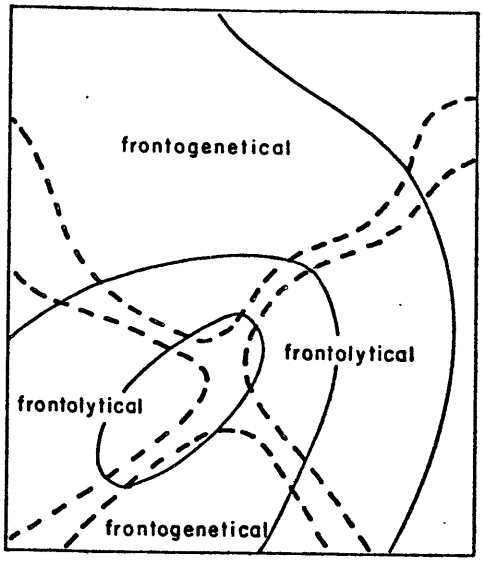

Figure 4.3 Frontogenetical and frontolytical areas due to horizontal geostrophic deformation associated with zipper low, derived from orientation of dilatation axes with respect to surface isotherms. (Solid lines represent isobars.)

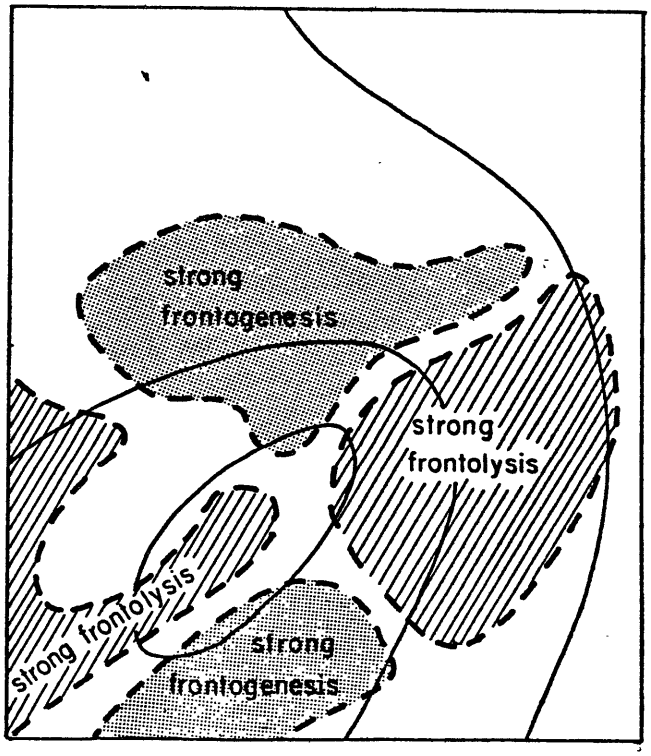

Figure 4.4 Frontogenetical field due to horizontal geostrophic deformation associated with zipper low. (Solid lines represent isobars.)

frontogenetical areas denote the regions where the angle between the axes and the isotherms is less than 40 degrees, while the frontolytical areas show where this angle is between 50 and 90 degrees. The neutral areas are where the angle is between 40 and 50 degrees, i.e. where the effect of geostrophic deformation is weak. (There is zero effect when the angle is 45 degrees.) The figure shows that the effect of geostrophic deformation is frontogenetical ahead and to the left of the low, as well as behind and to the right of it. Conversely, it is frontolytical ahead and to the right of the low, and behind to the left of it. It appears that the zipper effect of the cyclone is associated with the frontogenetical area ahead of the it. This may best be seen in Figure 4.4 which was derived by combining the effects of both magnitude and direction of the geostrophic deformation. The suggestion offered here is that the area of strong frontogenesis found ahead of the low is responsible for the intensification of the thermal gradient.

It is important to note that this simplified example involves the frontogenetical effect of horizontal geostrophic deformation in a field of uniform temperature gradient. (Note the even spacing of the isotherms in Figure 4.1.) A more realistic situation includes a stronger gradient along the coastline due to the land-sea thermal contrast. This would explain the tendency for the

strongest frontogenesis to occur on the right (or eastern) side of the frontogenetical region ahead of the low, as shown in Figure 4.4. The fact that this particular frontogenetical mechanism has such a relatively short time to act upon the boundary layer air emphasizes the importance of this pre-existing baroclinicity along the coast. Ahead of the low and away from the coast the deformation is strongly frontogenetical, but the initial temperature gradient here is typically weak so that the frontogenetical mechanism does not have enough time to increase the gradient to a significant intensity. Closer to the coast within the strong frontogenetical region, the initially stronger temperature contrast allows the geostrophic wind deformation field to increase the gradient to a more extreme intensity, as is manifested by the zipper effect of the surface cyclone.

Inspection of the zipper low case of 15 December 1981 verifies the diffluence in the isobars ahead of the cyclone at 0000 GMT, as well as the elongated shape of the low itself. Following the time series at 0600 GMT and 1200 GMT, it can be seen that these characteristics are maintained as the zipper low migrates northeastward. The strong temperature gradient that remains in wake of the passing cyclone is possibly due in part to the strong gradient of sea surface temperature that is present along the Atlantic seaboard. The eventual northward migration of

the ensuing surface cyclone in the path of the initial zipper low may also have an associated frontogenetical flow field ahead of it that would aid in the maintenance of this thermal gradient. By 1800 GMT, the zipper low begins to develop a more well-defined circulation, and the diffluence in the surface isobars just ahead of the it is not as apparent. A further deepening of the low will also serve to transform its shape from elongated to circular as the horizontal circulation becomes more organized. Such a deepening removes the geostrophically favorable mechanism responsible for the local strengthening of the thermal gradient, and is presumably responsible for the diminishing of the zipper effect of the low. At 1800 GMT the effect is still apparent in a pinching of the isotherms in the vicinity of the low, but the temperature gradient at the pinch is not as strong as it had been previously when the low was not as deep.

It should be noted here that the zipper effect of the cyclone is significantly altered by the shallow ocean water off the southeast coast of New England. This shallow ocean water is associated with a distinct cold region of sea surface temperature in this area. This alters the effect of the zipper low, as the air on the warm side of the front travels over this relatively cold ocean water and is cooled by conduction. This changes the shape of the surface isotherms, as the conductive cooling acts in opposition to

the advection of warm air. As the zipper low approaches this area, the cooled surface air on the warm side of the front cannot produce the intense strengthening of the surface air thermal gradient. This effect is illustrated in the case of 15 December at 1200 GMT when the surface cyclone is situated near Cape Cod, Massachusetts. Notice how the pinch in the isotherms (refer back to Figure 3.9) lags behind the low center, as the shape of the isotherms is affected by the relatively cold ocean water in the vicinity of the low. This cooling of the surface air by conduction is illustrated by the surface inversion in the Chatham (CHH) temperature sounding at 1200 GMT (Figure 4.5). The air temperature increases from 8.8°C at the surface to 10.4°C at 1000 mb, a vertical distance of just 74 meters. At 962 mb the temperature reaches 11.8°C. Therefore it is presumed that without the cooling by conduction of the cold water in this region, the surface air temperature gradient in the vicinity of the low at 12 GMT would have been more dramatic.

In light of the above description, the zipper low can now be compared to the cold anticyclone as a mechanism for the development of a coastal front. The initiation of coastal frontogenesis from the presence of a cold anticyclone can be viewed as a type of land breeze situation occurring when there is a large thermal contrast

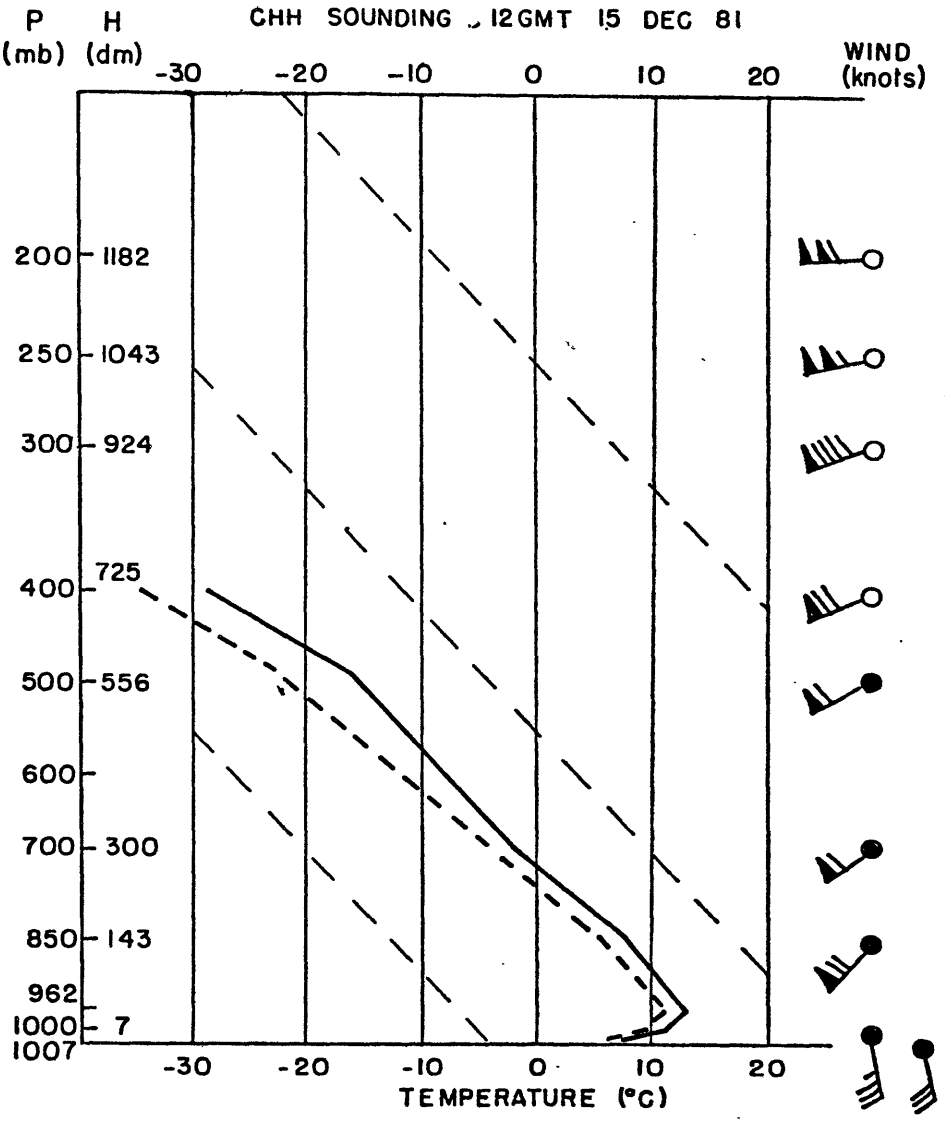

Figure 4.5 Temperature sounding from Chatham for 1200 GMT 15 December 1981.

between land and ocean. The land breeze is maximized when conduction following overnight radiational cooling of the surface increases the thermal contrast. When the geostrophic wind shifts to easterly or southeasterly over the ocean, the onshore flow converges at the coastline with the light northerly wind that is maintained inland. Heat fluxes from the relatively warm ocean diffuse into the air above and the warmer air is transported toward the coast where the thermal gradient intensifies. The result is a coastal front situation in which the wind on either side of the front has a large component normal to the front, in response to the intense thermal contrast. Differential surface friction at the coast aids in the development of the front, but the tendency for the front to creep slowly inland indicates an encroachment onto land of the heat that has been supplied by the relatively warm ocean and transported landward. Such an inland migration of the front cannot be explained by differential friction (since the coast certainly does not migrate) and this implies that the importance of differential surface friction lies more in the initiation of the front, rather than its maintenance. The eventual dissipation of the coastal front occurs with the passing of a deepening surface cyclone. The cyclone presumably plays no role in the initiation of the front as frontogenesis occurs well ahead of it, but the approach of the developing cyclone increases the

geostrophic onshore flow which brings a greater flux of heat to the coast to intensify the frontal zone. As the cyclone passes, its circulation envelopes the frontal zone and removes it from the coast, and the strength of the front weakens as it moves out over the ocean. The weakening of the frontal zone over the ocean is difficult to verify due to the sparse data availability, but the limited evidence suggests this is true, and the removal of the front from the region of differential surface friction would certainly support it theoretically.

As described earlier, the air flow associated with the cold anticyclone coastal front is essentially normal to the front. Warm air is entrained into the frontal zone at the surface and trajected upward, as in the intense surface front described by Sanders (1955). Such a process requires the constant renewal of a warm air supply to the surface frontal zone, which is provided by the onshore geostrophic flow over the warm ocean water. The frontogenetical process associated with the zipper low differs in that the flow of air is more parallel to the frontal zone, and therefore the entrainment process is not as strong. The coastal front in this instance becomes more of a boundary between two distinct "masses" of air; the air on either side of the front has a trajectory which allows it to remain within its respective mass for an extensive period of time instead of flowing directly into the frontal zone

and mixing through turbulent processes

In contrast to the cold anticyclone coastal front, the zipper low is responsible for the strengthening of a frontal zone that results from small synoptic scale geostrophic forcing, as indicated by the frontogenetically favorable deformation field that accompanies it. The fact that that the frontal zone often is strongest to the east of this deformation maximum indicates the tendency for the process to take advantage of the thermal gradient provided by the land-sea temperature contrast along the coast. This geostrophic forcing remains distinctly associated with the migrating low, which allows for the local strengthening of the temperature gradient in the vicinity of the cyclone. This is not to say that the frontal zone is transported by the cyclone, but instead that the frontogenetical process accompanies the cyclone. Such a process is not apparent in coastal frontogenesis initiated by a cold anticyclone, which explains the tendency for the frontal zone to stagnate in one location.

Observations from a variety of cases allows for a general description of the conditions associated with zipper low frontogenesis. The central pressure is usually greater than 1000 mb, and it has been observed to be as high as 1015 mb. These cyclones are often very rapid movers and are subject to downstream re-development, and are many times associated with a series of lows that follow

similar paths. Like the surface cyclones which dissipate the cold anticyclone coastal front, they tend to travel along the baroclinic zone that constitutes the front. Because the frontal zone remains in their wake, they result in long stretches of baroclinicity and are associated with very widespread (and sometimes patchy) areas of precipitation with largest amounts falling in regions that remain in the baroclinic zone for extended periods of time. Synoptically, they are sometimes, but not always, found to form in the southeastern United States when there is an anticyclone situated in the western Atlantic Ocean that provides a southerly geostrophic flow parallel to the Atlantic coastline. Because the geostrophic flow is parallel to the coastal front, the effect of differential diabatic heating from oceanic heat fluxes is presumably less significant than it is for the coastal front initiated by a cold anticyclone with strong onshore flow. Finally, the cyclone usually has an elongated shape that is able to maintain its zipper effect for up to a couple of days. The eventual deepening of the cyclone increases the circulation around the low center, and is assumed to be responsible for the removal of the zipper effect.

5.0 Conclusion

Two distinct mechanisms for the initiation and development of coastal frontogenesis have been compared and contrasted. Coastal fronts forming to the south of a cold anticyclone tend to stagnate in one location, and they exhibit airflow that is basically normal to the front. The approach of a deepening coastal cyclone aids in the intensification of the frontal zone due to increased onshore flow, but the presence of the coastal low is not crucial to the initial establishment of the front. Passage of the cyclone results in a weakening and removal of the front from the coast, and an abrupt cessation of precipitation. Precipitation amounts are found to be correlated with the areas of strongest horizontal thermal gradient. Frontogenesis induced by the zipper low relies on a weak, slowly deepening surface cyclone that produces a local strengthening of the temperature gradient. Unlike the cold anticyclone coastal front, the synoptic scale horizontal geostrophic deformation associated with the zipper low appears to play a positive role in frontogenesis. The cyclone is usually elongated in shape, and provides an airflow that is more parallel to the front. The frontal zone remains distinct along the coast after the passage of the zipper low. The zipper effect presumably diminishes as a result of the eventual deepening of the

cyclone which causes a more intense circulation.

Aspects of the coastal front not considered in detail here are presently subject to further research. The vertical structure of coastal fronts established by a cold anticyclone is becoming better understood through the use of data from airplanes that have traversed the frontal zone at various levels. Numerical modeling to improve upon the work of Ballentine is also being developed. A more detailed analysis of the zipper low case of 15 December 1981 is near completion at this writing. The suggestion of a more rigorous climatological study of the zipper low is offered here. An improvement in the surface observations over the ocean for use in coastal front research is also suggested. Since the coastal front is a lower boundary layer phenomenon, research may become more fruitful through the development of a mesoscale surface observation network that will provide more and better data over the ocean where data availability at this time is sparse and less reliable. With the recent acquisition of coastal front information from airplane data, an improvement in the surface observing network would act as a useful supplement and provide a base for more comprehensive observational coastal front research.

Appendix: Frontogenesis Calculations for 23-24 JAN 82

Extraordinarily intense surface horizontal thermal gradients were observed along the New England coastline during the case of 23-24 January 1982, as documented in this paper. Calculations have been carried out in order to test the response of the horizontal temperature field to the frontogenetical forcing by the observed wind.

The temporal rate of change of potential temperature following a parcel can be written (as from Anthes et al., 1982, Bosart, 1970, and Miller, 1948) as:

$$\frac{d}{dt}\left|\nabla_p \theta\right| = \left|\nabla_p \theta\right|^{-1}\left\{-\left[\left(\frac{\partial\theta}{\partial x}\right)^2\frac{\partial u}{\partial x}+\left(\frac{\partial\theta}{\partial y}\right)^2\frac{\partial v}{\partial y}\right]-\frac{\partial\theta}{\partial x}\frac{\partial\theta}{\partial y}\left(\frac{\partial v}{\partial x}+\frac{\partial u}{\partial y}\right)\right.$$
$$\left.-\left[\left(\frac{\partial\theta}{\partial x}\frac{\partial\theta}{\partial p}\right)\frac{\partial\dot{p}}{\partial x}+\left(\frac{\partial\theta}{\partial y}\frac{\partial\theta}{\partial p}\right)\frac{\partial\dot{p}}{\partial y}\right]+\left[\frac{\partial\theta}{\partial x}\frac{\partial}{\partial x}\left(\frac{d\theta}{dt}\right)+\frac{\partial\theta}{\partial y}\frac{\partial}{\partial y}\left(\frac{d\theta}{dt}\right)\right]\right\}$$

where x and y are directed toward the east and north respectively, and the other symbols have their conventional meteorological meaning. The first term on the right hand side of the equation describes the effect of confluence by the horizontal wind, the second term describes the effect of horizontal shear, the third term is the frontogenesis due to vertical advection, and the fourth term is the frontogenetical rate due to differential diabatic heating. We are interested in the effects of horizontal advection near the surface, so the equation can be simplified using

the confluence and shearing terms:

$$\frac{d}{dt}\left|\nabla_H T\right| = \left|\nabla_H T\right|^{-1}\left\{\left[\left(\frac{\partial T}{\partial x}\right)^2\frac{\partial u}{\partial x} + \left(\frac{\partial T}{\partial y}\right)^2\frac{\partial v}{\partial y}\right] - \frac{\partial T}{\partial x}\frac{\partial T}{\partial y}\left(\frac{\partial v}{\partial x} + \frac{\partial u}{\partial y}\right)\right\}$$

This frontogenetical rate was calculated at the key sites indicated in Figure 2.2, using centered finite differencing across a horizontal length of 1 degree latitude. Actual horizontal temperature gradients were calculated in the same manner. The actual temperature gradient was also calculated on a smaller scale between station pairs located along the coastline that roughly correspond to the coastal sites E through I. The results are summarized in the following tables. Temperature gradients are given in units of C/100 km and frontogenesis rates are in C/100 km/3 hours. Values in parentheses are estimates:

Site A (Land)

Time	Actual $\lvert\nabla_H T\rvert$	Actual $\frac{\partial}{\partial t}\lvert\nabla_H T\rvert$	Calculated $\frac{d}{dt}\lvert\nabla_H T\rvert$
23 JAN			
12 GMT	3.3		
		-1.2	-0.6
15	2.1		
		2.2	-0.5
18	4.3		
		6.4	-2.1
21	10.7		
24 JAN		-1.8	2.3
00 GMT	8.9		
		-3.1	-2.1
03	5.8		
		2.6	1.9
06	8.4		
		1.2	6.1
09	9.6		

Site B (Land)

Actual $\lvert\nabla_H T\rvert$	Actual $\frac{\partial}{\partial t}\lvert\nabla_H T\rvert$	Calculated $\frac{d}{dt}\lvert\nabla_H T\rvert$
1.1		
	0.0	-0.3
1.1		
	0.0	0.2
1.1		
	1.4	-0.7
2.5		
	0.7	-1.2
3.2		
	-1.0	0.3
2.2		
	1.6	0.5
3.8		
	-2.7	1.0
1.1		

Site C (Land)

23 JAN			
12 GMT	4.9		
		-3.9	-1.7
15	1.0		
		-0.3	-0.2
18	0.7		
		1.4	0.2
21	2.1		
24 JAN		0.5	0.4
00 GMT	2.6		
		1.2	0.2
03	3.8		
		-1.7	-1.2
06	2.1		
		2.3	0.0
09	4.4		

Site D (Land)

5.2		
	-0.2	-0.7
5.0		
	-1.3	-1.1
3.7		
	0.0	-1.3
3.7		
	2.7	-2.5
6.4		
	0.8	2.1
7.2		
	-0.7	1.0
6.5		
	-1.9	0.1
4.6		

	LARGER SCALE			SMALLER SCALE	
	Site E (Coast)			BGR-Great Duck (Δn=89 km)	
Time	Actual $\lvert\nabla_h T\rvert$	Actual $\frac{\partial}{\partial t}\lvert\nabla_h T\rvert$	Calculated $\frac{d}{dt}\lvert\nabla_h T\rvert$	Actual $\lvert\nabla_h T\rvert$	Actual $\frac{\partial}{\partial t}\lvert\nabla_h T\rvert$
23 JAN					
12 GMT	10.1			8.7	
		-2.4	-0.4		-3.1
15	7.7			5.6	
		2.8	1.2		5.6
18	10.5			11.2	
		1.8	5.9		2.5
21	12.3			13.7	
24 JAN		-2.1	14.8		-0.6
00 GMT	10.2			13.1	
		-0.3	16.9		-1.9
03	9.9			11.2	
		-4.5	12.4		-6.2
06	5.4			5.0	
		8.1	6.4		9.3
09	13.5			14.3	

	Site F (Coast)			NHZ-Seguin (Δn=28 km)	
23 JAN					
12 GMT	13.9			25.8	
		-0.8	4.9		-4.0
15	13.1			21.8	
		3.5	5.4		19.9
18	16.6			41.7	
		4.9	16.5		5.9
21	21.5			47.6	
24 JAN		0.2	45.4		4.0
00 GMT	21.7			51.6	
		-1.4	53.8		-3.9
03	20.3			41.7	
		-4.4	43.3		-23.9
06	15.9			17.8	
		-4.0	8.9		-11.9
09	11.9			5.9	

LARGER SCALE

SMALLER SCALE

Site G (Coast)

PWM-Wood (Δn=21 km)

Time	Actual $\lvert\nabla_n T\rvert$	Actual $\frac{\partial}{\partial t}\lvert\nabla_n T\rvert$	Calculated $\frac{d}{dt}\lvert\nabla_n T\rvert$	Actual $\lvert\nabla_n T\rvert$	Actual $\frac{\partial}{\partial t}\lvert\nabla_n T\rvert$
23 JAN					
12 GMT	15.8			34.4	
		1.1	11.7		-21.2
15	16.9			13.2	
		0.8	13.8		2.7
18	17.7			15.9	
		4.3	28.0		47.6
21	22.0			63.5	
24 JAN		-1.4	44.6		0.0
00 GMT	20.6			63.5	
		2.4	53.4		(21.2)
03	23.0			(42.3)	
		-11.2	48.1		(-38.0)
06	11.8			(5.3)	
		-0.5	-4.7		(0.0)
09	11.3			(5.3)	

Site H (Coast)

PSM-Shoals (Δn=19 km)

23 JAN					
12 GMT	12.9			38.0	
		0.5	6.3		11.7
15	13.4			49.7	
		2.9	9.7		8.8
18	16.3			58.5	
		0.0	23.6		5.8
21	16.3			64.3	
24 JAN		-1.5	27.3		-29.2
00 GMT	14.8			35.1	
		2.3	8.9		23.4
03	17.1			58.5	
		-9.2	15.3		-46.8
06	7.9			11.7	
		0.3	-3.8		14.6
09	8.2			26.3	

LARGER SCALE

SMALLER SCALE

Site I (Coast)

OWD-Scituate (Δn=49 km)

Time	Actual $\lvert\nabla_H T\rvert$	Actual $\frac{\partial}{\partial t}\lvert\nabla_H T\rvert$	Calculated $\frac{d}{dt}\lvert\nabla_H T\rvert$	Actual $\lvert\nabla_H T\rvert$	Actual $\frac{\partial}{\partial t}\lvert\nabla_H T\rvert$
23 JAN					
12 GMT	6.5			12.4	
		2.2	2.2		0.0
15	8.5			12.4	
		-6.7	1.9		-10.1
18	1.8			2.3	
		2.3	0.9		0.0
21	4.1			2.3	
24 JAN		0.9	3.3		2.2
00 GMT	5.0			4.5	
		1.8	3.2		3.4
03	6.8			7.9	
		-1.4	4.0		(2.3)
06	5.4			(10.2)	
		-0.7	-1.8		(3.4)
09	4.7			(13.6)	

Site J (Ocean)

Time	Actual $\lvert\nabla_H T\rvert$	Actual $\frac{\partial}{\partial t}\lvert\nabla_H T\rvert$	Calculated $\frac{d}{dt}\lvert\nabla_H T\rvert$
23 JAN			
12 GMT	6.3		
		-0.5	1.6
15	5.8		
		-0.9	1.6
18	4.9		
		-1.6	-1.9
21	3.3		
24 JAN		0.3	-0.3
00 GMT	3.6		
		1.0	1.8
03	4.6		
		-1.5	1.7
06	3.1		
		-2.0	0.2
09	1.1		

	Site K (Ocean)			Site L (Ocean)		
	Actual	Actual	Calculated	Actual	Actual	Calculated
Time	$\lvert\nabla_H T\rvert$	$\frac{\partial}{\partial t}\lvert\nabla_H T\rvert$	$\frac{d}{dt}\lvert\nabla_H T\rvert$	$\lvert\nabla_H T\rvert$	$\frac{\partial}{\partial t}\lvert\nabla_H T\rvert$	$\frac{d}{dt}\lvert\nabla_H T\rvert$
23 JAN						
12 GMT	5.5			2.6		
		-1.4	0.0		-1.9	-0.2
15	4.1			0.7		
		-3.0	2.7		0.8	0.0
18	1.1			1.5		
		0.7	0.5		-1.5	-0.3
21	1.8			0.0		
24 JAN		-0.3	-0.9		1.1	0.0
00 GMT	1.5			1.1		
		-0.4	0.2		2.8	0.3
03	1.1			3.9		
		10.1	0.8		-0.9	-0.1
06	11.2			3.0		
		-2.7	4.2		-1.4	-0.9
09	8.5			1.6		

Inspection of the calculations reveals that there is not an impressive correlation between the sign of the actual and calculated frontogenetical rates for the land and ocean sites where the temperature gradients are relatively small and are not necessarily being dominated by the horizontal advection terms. Along the coast, however, the frontogenetical rates calculated from the observed horizontal wind do correspond, in sign, to the observed intensification of the frontal zone. As expected, the calculated rates are much greater than the actual rates since they do not include the frontolytical effect of turbulent mixing. Since the frontal zone is occurring on such a small width scale, the actual frontogenetical rates for the smaller scale station pairs more closely correspond to the large calculated values. The frontogenetical

contribution by the horizontal advection terms reaches a maximum approximately three to six hours after the time of maximum actual frontogenesis. This can be seen in the following table:

		Time of Maximum $\lvert\nabla_H T\rvert$ (GMT)	Time of Maximum $\frac{\partial}{\partial t}\lvert\nabla_H T\rvert_{actual}$ (GMT)	Time of Maximum $\frac{d}{dt}\lvert\nabla_H T\rvert_{calculated}$ (GMT)
Site E	Larger Scale	2100	1500-1800	0000-0300
	Smaller Scale	2100	1500-1800	
Site F	Larger Scale	0000	1800-2100	0000-0300
	Smaller Scale	0000	1500-1800	
Site G	Larger Scale	0300	1800-2100	0000-0300
	Smaller Scale	2100, 0000	1800-2100	
Site H	Larger Scale	2100	1500-1800	2100-0000
	Smaller Scale	2100	0000-0300	
Site I	Larger Scale	1500	1800-2100	0300-0600
	Smaller Scale	1200, 1500	0000-0300	

Acknowledgements

I would like to thank Professor Frederick Sanders for his continual guidance throughout the course of this work, as well as for his inspirational enthusiasm for synoptic meteorology in general. I wish to express appreciation for the companionship and support of my friends at M.I.T. Thanks go to Brad Colman for his stabilizing influence on all of us, and without whose acknowledgement no thesis is complete. Thanks also go to Isabelle Kole for her help in drafting the figures.

This work was funded by the National Science Foundation under Grants ATM-8013711 and ATM-8209375.

And finally, I would like to dedicate this thesis to my father, who would like to have seen it more than anyone.

References

Anthes, Kuo, Benjamin, and Li, 1982: "The evolution of the mesoscale environment of severe local storms: Preliminary modeling results." Monthly Weather Review, Volume 110, 1187-1213.

Baker, D.G., 1970: "A study of high pressure ridges to the east of the Appalachian Mountains." Ph.D. Thesis, Department of Meteorology, M.I.T., 127 pages.

Ballentine, R.J., 1980: "A numerical investigation of New England coastal frontogenesis." Monthly Weather Review, Volume 108, 1479-1497.

Bergeron, T., 1928: "Über die dreidimensional verknüpfende Wettranalyse I." Geofys. Publikasjoner, Volume 5, Number 6, 1-111.

Bosart, L.F., 1970: "Mid-tropospheric frontogenesis." Quarterly Journal of the Royal Meteorological Society, Volume 96, 442-471.

Bosart, L.F., 1972: "Coastal frontogenesis." Journal of Applied Meteorology, Volume 11, 1236-1258.

Bosart, L.F., 1975: "New England coastal frontogenesis." Quarterly Journal of the Royal Meteorological Society, Volume 101, 957-978.

Hoskins, B.J., and F.P. Bretherton, 1972: "Atmospheric frontogenesis models: Mathematical formulation and solution." Journal of the Atmospheric Sciences, Volume 29, 11-37.

Lettau, H.H., and W.F. Dabberdt, 1970: "Variangular wind spirals." Boundary Layer Meteorology, Volume 1, 64-79.

Marks, F.D., Jr, 1975: "A study of the mesoscale precipitation associated with the New England coastal Front." Ph.D Thesis, Department of Meteorology, M.I.T., 85 pages.

Marks, F.D., Jr., 1979: "Effects of the New England coastal front on the distribution of precipitation." Monthly Weather Review, Volume 107, 53-67.

Miller, J.E., 1948: "On the concept of frontogenesis." Journal of Applied Meteorology, Volume 5, 169-171.

Petterssen, S., 1956: Weather Analysis and Forecasting, Volume 1, 2nd Edition, McGraw-Hill, N.Y., Chapter 11.

Sanders, F., 1955: "Investigation of the structure and dynamics of an intense surface frontal zone." Journal of Meteorology, Volume 12, 542-552.

Saucier, W.J., 1955: Principles of Meteorological Analysis, University of Chicago Press, Chicago.

Stone, P.H., 1966: "Frontogenesis by horizontal wind deformation fields." Journal of the Atmospheric Sciences, Volume 23, 455-465.